EXPERIMENTAL AND THEORETICAL EVALUATION OF THE FILTRATION MECHANISMS FOR A MAGNETIC SEPARATIONS PROCESS

A Thesis
Presented to the
The Academic Faculty

by

Jeremy S. Noonan

In Partial Fulfillment
Of the Requirements for the Degree
Master of Environmental Engineering in the
School of Civil and Environmental Engineering

Georgia Institute of Technology
April 2005

EXPERIMENTAL AND THEORETICAL EVALUATION OF THE FILTRATION MECHANISMS FOR A MAGNETIC SEPARATIONS PROCESS

Approved by:

Dr. Costas Tsouris, Advisor

Dr. Sotira Yiacoumi

Dr. Jaehong Kim

Date Approved

April 12, 2005

ACKNOWLEDGEMENTS

I would first like to thank the professors and research scientists who guided me through this process. I thank Dr. Costas Tsouris for giving me the opportunity to work on this project and advising me along the way. I thank Dr. Sotira Yiacoumi for first inviting me to work on this project. I thank Drs. Kurt Pennell, Mark White (ChE), and Mark Prausnitz (ChE) for their helpful discussions about surface chemistry and experimental design. I thank Dr. James Amburgey for taking the time to help me understand filtration theory through his very thorough emails. And I thank Dr. Guangxuan Zhu for his steady help throughout this project, especially for teaching me how to use the Atomic Absorption Spectrometer.

I would also like to acknowledge my fellow students who helped. I thank Patricia Taboada-Serrano for teaching me about DLVO theory and force potential curves. I thank Jed Costanza for helping me to setup my filtration column correctly, and for our encouraging discussions about research. And I thank my other group members, Viriya Vithayaveroj and Chiahung Hou, for answering my questions about the lab and putting up with all of the noise my experiments made. I especially thank Justin Clark for helping me in the lab with experiments.

The Environmental Engineering support staff also deserve recognition. I thank Andrea Be and Therese Rehkopf for their cheerful, reliable support with paperwork and ordering supplies.

I thank my wife Kelly who has encouraged me and has worked hard to support me in graduate school. And thanks be to the God of Abraham from whom all blessings flow.

TABLE OF CONTENTS

LIST OF TABLES

LIST OF FIGURES

LIST OF SYMBOLS

a	Wire radius (m)
b	Particle radius (m)
B_o	Magnitude of applied magnetic induction (T)
Cin	Influent concentration (M)
Cout	Effluent concentration (M)
G	Gravitational force parameter
g	Gravitational acceleration (m s^{2-})
H_o	Magnitude of the external magnetic field strength (A m^{-1})
$\mathbf{F_m}$	Magnetic Force (N)
$\mathbf{F_d}$	Drag Force (N)
$\mathbf{F_g}$	Gravitational Force (N)
k	Boltzmann constant (J/K)
L	Filter length (m)
M	Magnetization (A m^{-1})
M_s	Saturation magnetization (A m^{-1})
R	Normalized radius
R_c	Critical radius
RE	Removal efficiency
$\Re$	Reynolds number
r	Center-to-center particle separation (m)
T	Temperature (K)
V_o	Magnitude of superficial fluid velocity (m/s)

V_m Magnetic velocity (m/s)

V_r Radial superficial fluid velocity (m/s)

$V_{\square}$ Tangential superficial fluid velocity (m/s)

V_{pr} Radial particle velocity (m/s)

$V_{p\square}$ Tangential particle velocity (m/s)

η Collision efficiency factor

β Angle between x-axis and gravity vector

γ Angle between x-axis and fluid velocity vector

ε Porosity of the filter (dimensionless)

η Fluid dynamic viscosity (in magnetic filtration model) or collector efficiency (in non-magnetic filtration model) (kg/m-s)

θ Tangential component

μ Fluid dynamic viscosity (in non-magnetic filtration model) (kg/m-s)

μ_0 Permeability of free space (H/m)

ρ_f Fluid density (kg/m^3)

ρ_p Particle density (kg/m^3)

χ_p volume magnetic susceptibility (dimensionless)

SUMMARY

High-Gradient Magnetic Separation (HGMS) is a powerful separation process that has great potential for industrial wastewater treatment, particularly for the removal and recovery of paramagnetic colloidal particles. HGMS relies primarily on a magnetic force as the mechanism for the capture of particles on collectors. The chief advantages of HGMS are that the separation is reversible and potentially selective. The separation is reversible because the magnetic force can be disabled at any time, allowing for efficient filter regeneration. The separation is selective because it only removes those particles that are susceptible to a magnetic force and the efficiency of removal depends largely on the degree of this susceptibility. This property allows for the potential recovery and reuse of valuable waste materials. These advantages, however, are null if there are other significant attractive forces between the particle and collector that can cause non-reversible and non-selective separation.

The objective of this study was to identify the chief mechanisms responsible for the removal of ferric oxide (Fe_2O_3) from water by an HGMS process. This objective was achieved by measuring the effects of applied magnetic induction, collector radius, and fluid velocity on the removal efficiency (RE) of a stainless-steel filter column. These factors were tested on the removal of bare Fe_2O_3 particles and particles treated with a surfactant (sodium dodecyl sulfate, SDS). The results were compared to the predictions of a trajectory model which simulates particle capture by a magnetic force.

The experimental results show that non-magnetic force mechanisms are primarily responsible for the removal of bare Fe_2O_3 particles for the experimental conditions used in this work. For these particles, the three factors tested had no significant effect on the

RE, and 90.1% of the particles were removed without a magnetic force. These results differed sharply from modeling predictions. However, the magnetic force mechanism is primarily responsible for the removal of surfactant-treated Fe_2O_3 particles. The three factors investigated had a marked effect on the RE, and only 10.8% of the particles were removed without a magnetic force. An increase in magnetic induction from 0.2 to 0.5 T increased the RE from 79.9 to 93.4 %; a decrease in wire radius from 49 to 15 μm increased the RE from 60.2 to 93.4%, and a decrease in fluid velocity from 0.5 to 0.1 cm/s increased the RE from 69.5 to 95.3%. These results agreed closely with the model predictions.

These results indicate the surfactant-treatment has a negative effect on removal efficiency. Other measurements show, however, that surfactant-treatment has a positive effect on particle recovery and filter regeneration. Nearly 90% of SDS-treated particles were recovered from the filter immediately after shutting down the magnetic field, while only 30% of bare particles were recovered.

Additional tests were performed treating the particles with other types of surfactants. These surfactants (CTAB and Tween 80) had no effect on the RE with a magnetic force, but in the absence of a magnetic force, the RE was 5.9% and 14.7% for CTAB and Tween 80, respectively. These results suggest that other surfactants might improve the selectivity of the separation by enhancing particle stability.

This study demonstrates that by reducing the effect of attractive non-magnetic forces on filtration, surfactant treatment of colloidal particles can potentially preserve and enhance these two key advantages, i.e., regeneration and selectivity of HGMS processes.

CHAPTER 1

INTRODUCTION

Filtration is the earliest method of water treatment practiced by man. As evidenced by Egyptian and Sanskrit inscriptions, water was treated using filtration as early as 200 B.C. (Baker, 1949). Perhaps filtration was discovered and used early in the history of civilization because it is a natural separation process, simulating the way the earth removes contaminants from water, by taking advantage of attractive forces between particulate matter suspended in the water and the surface of the filter media.

Filtration processes have become more sophisticated and better engineered over time, but this basic principle remains the same: the effectiveness of a filtration process depends on the interplay of forces between the contaminants to be removed and the filter media. The degree to which the attractive forces dominate the repulsive forces determines how efficiently the filter will remove the contaminants.

Since the advent of the industrial revolution, increasing amounts of man-made metallic waste have been discharged into rivers, lakes, and oceans around the world. In response to this industrial pollution, governments are passing increasingly stringent requirements for wastewater treatment, and punish companies with heavy fines if their factories' waste streams fail to meet these requirements. Thus, industries have had to find increasingly effective separation processes for treating their waste streams. According to the basic principle of filtration, one way to improve separation processes is to strengthen the attractive force between contaminants and filter medium. This strategy underlies the development of magnetic filtration as a useful method for more effective water and wastewater treatment.

Magnetic filtration employs a magnetic force as a mechanism to attract contaminants to the filter medium, thereby removing them from wastewater. Thus, the effectiveness of the filtration process is related directly to the strength of the magnetic force. The strength of the magnetic force is determined by factors associated with the physical properties of the particle (volume and magnetic susceptibility) and with the intensity of the magnetic field gradient around the wire collectors, quantified as the magnetic field density (Gerber and Birss, 1983). Originally, magnetic filters could only generate a low intensity field density. Thus, the application of this technique was limited to removing large, highly magnetic particles, such as ferromagnetic particles, which are very susceptible to a magnetic field. However, the range of potential applications broadened with the development of high-gradient separation (HGMS).

By increasing the magnetic field gradient around the filter media, HGMS can capture smaller (micron-sized) particles that are only weakly magnetic (paramagnetic), thus expanding the range of applications of magnetic filtration. Used widely in the steel and mineral processing industries, HGMS also has many potential wastewater treatment applications. Researchers have shown HGMS to be effective for the removal of phosphates and sludge from water (Shaikh and Dixit, 1992; Barrado, 1999), the recovery of radionucleotides (Bahaj, 1998), and the separation of heavy metals (Anand, 1985). Coupled with novel techniques like magnetic seeding in which magnetic particles flocculate with non-magnetic particles, and functionalized particles in which magnetic particles are designed to have a specific affinity for non-magnetic contaminants, HGMS may also be used to remove synthetic organic compounds (Moeser et al., 2002), biomolecules (Bucak et al., 2003), ferrihydrate (Karapinar, 2003), and heavy metals

(Phanapavudhikul et al., 2003; Kaminiski and Nunez, 1999). Indeed, HGMS holds promise for the removal of any paramagnetic micron-size contaminant from wastewater.

When evaluating whether HGMS should be implemented to improve the separation of paramagnetic micron-sized particles, one should first determine whether magnetic filtration results in superior removal efficiency over non-magnetic (mechanical) filtration. If magnetic filtration achieves superior removal over alternative methods, then the next step is to design a process in which the removal efficiency is maximized. To design an optimal process, it is necessary to know the key design factors that determine the performance of the process and how these factors affect the performance. The ability of a magnetic filtration process to retain particles, like any other filtration process, depends on a competition between attractive and repulsive forces. Thus, the key design factors are those parameters which influence the magnitude of the forces at work in the process. By manipulating these parameters, one can alter the balance of forces to maximize the attractive forces while minimizing the repulsive forces. If one had a model that simulated accurately the interaction of these forces, it would be possible to predict the effect the parameters that govern these forces have on the performance of an HGMS process. Such a model would be useful for designing a magnetic filtration process by guiding the selection of the levels of the parameters that will optimize the process.

Since the introduction of HGMS in the late 1960s, numerous efforts have been made to model the performance of magnetic filters. A commonly used indicator of filter performance is the removal efficiency (RE), which is derived from the ratio of the concentration of the contaminant in the effluent to the concentration in the feed. Trajectory models, which simulate the influence of various forces on the interaction

between a single particle and a single wire collector, have been used to predict the effect of key design factors on the capture cross section for a clean filter (Watson 1973; Lawson, Simons, & Treat 1977; Ebner, A.D. and Ritter, J.A. 1997, 2001). Buildup models, which account for changes in the surface characteristics of the filter wire due to particle deposition and thus consider the contribution of inter-particle forces, have been used to predict the loading volume of a filter (Luborsky and Drummond 1976; Nesset and Finch 1981). The loading volume is useful for estimating another important indicator of filter performance – the time until breakthrough concentration occurs in the effluent. Incorporating the trajectory and buildup models into a population-balance model, Ying et al. (2000) developed a breakthrough model that predicts effluent concentration versus time for a HGMS process coupled with magnetic seeding, and showed a close agreement between model predictions and experimental results of effluent concentration versus time.

This good agreement between modeling and experimental results indicates that this model may be useful for designing magnetic filtration processes. However, this model was only tested experimentally for the filtration of two types of particles by one type of filter medium. With a different type of particle and filter medium, there may be other mechanisms affecting filtration. If there are other mechanisms, the forces that influence them should also be incorporated into the model. The purpose of this study is to experimentally identify the mechanisms that influence the performance of an HGMS filter, and to quantify the effects of the parameters that determine the magnitude of two of the major forces that affect these mechanisms. If we understand the major mechanisms and how the design parameters affect the mechanisms, we can then evaluate the quality

of the model and identify ways to improve it by building into it the relevant parameters. With such a model, we could predict accurately the effects of key design parameters, and thus design a magnetic filter to optimize its effectiveness.

The effectiveness of a separation process is chiefly evaluated by the efficiency of removal. However, there are other criteria that must also be considered when evaluating performance. One is the ease of regeneration. As particles build-up in the filter, the filter becomes clogged and the removal efficiency decreases. Consequently, the filter must be periodically washed to remove the particles. This regeneration process can be time consuming, and so increase process costs. A related criterion is the recoverability of particles. In industrial wastewater treatment, the goal is often to not only remove particles, but also recover them for reuse. Both filter regeneration and particle recovery are easier to achieve if the separation is reversible. Reversibility of the separation can be achieved if the force responsible for removal can be nullified. The forces behind non-magnetic mechanisms are difficult to nullify, but a major advantage of a magnetic separation mechanism is that it is easy to nullify the magnetic force. If we know which mechanisms are responsible for removal, then we can also assess a filter's effectiveness by these criteria.

This study examines the effect of applied magnetic induction, fluid velocity, and collector thickness on the removal of bare paramagnetic ferric oxide (Fe_2O_3) particles and surfactant-treated Fe_2O_3 particles from water by a stainless steel wool filter. The study shows that non-magnetic filtration mechanisms govern the removal of bare Fe_2O_3 particles. However, when the operation of these non-magnetic mechanisms is severely dismantled by treating Fe_2O_3 particles with a surfactant, the magnetic filtration

mechanism governs particle removal. Consequently, the model better predicts the removal of surfactant-treated particles, and these particles are easier to recover from the filter.

CHAPTER 2

THEORY

2.1 Magnetic Filtration Mechanism

The ultimate goal of a mathematical model for a magnetic filtration process is to predict filter performance as a function of key design parameters. In this study, filter performance is measured primarily by removal efficiency (RE). Thus, the model predicts the removal efficiency for clean magnetic filter. This prediction is based on a balance of the major forces that determine the path of a single particle with respect to a single wire collector. Hence, the model is referred to as a "trajectory model." Trajectory models have been used extensively to analyze the efficiency of non-magnetic filtration using granular filter media. The application of trajectory analysis to filtration originated with the work of Sell (1931) and Albricht (1931) on aerosol deposition. This work was extended to hydrosol deposition by O'Melia and Strumm (1967), Yao (1968), Yao et al (1971), Rajagopalan and Tien (1977), and Payatakes et al. (1974). The popular use of trajectory analysis for non-magnetic filtration inspired the development of trajectory modeling for magnetic filtration.

The forces included in this model are the magnetic force ($\mathbf{F_m}$), the drag force ($\mathbf{F_d}$), and the gravitational force ($\mathbf{F_g}$). Each force is resolved into two components, a radial (r) and a tangential (θ). These correspond to a polar coordinate system (Figure 1), onto which the motion of the particle is mapped.

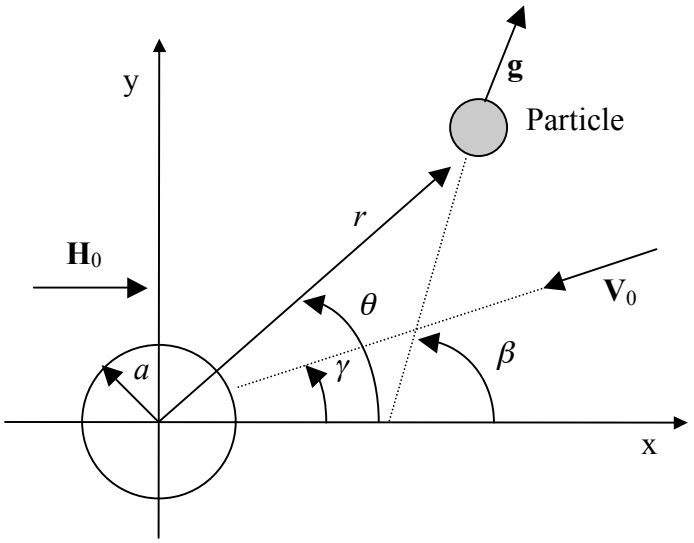

Figure 1: Polar coordinate system for mapping particle trajectory with reference to a single wire. $\mathbf{H}_0$ is the external magnetic field, $\mathbf{V}_0$ is the fluid velocity, a is the wire radius, and $\mathbf{g}$ is gravity (Ying, 2000).

Magnetic Force

The magnetic force acting on a particle can be described mathematically as (Ying, 2000):

$$\mathbf{F}_m = -\frac{4\pi b^3 \mu_0 \chi_p M H_0}{3a}\left[\bar{\mathbf{i}}_r\left(\frac{M}{2H_0 R^5}+\frac{\cos 2\theta}{R^3}\right)+\bar{\mathbf{i}}_\theta \frac{\sin 2\theta}{R^3}\right] \quad (1)$$

Where b is the particle radius, μ_0 (= $4\pi\times10^{-7}$ H m^{-1}) is the permeability of free space, χ_p is the volume magnetic susceptibility of a particle, M is the magnetization of the collector, Ho is the applied magnetic field strength, and a is the wire diameter. R is the distance between the center of the wire collector and the center of the particle, normalized to the wire diameter ($R = r/a$), and □ is the angle between the horizontal axis and r. This

equation shows that the magnetic force is a function of several parameters, two of which were studied experimentally in the present work. According to this equation, the magnetic force increases with the magnetic field strength, magnetization of the collector, and the magnetic susceptibility of the particle; it decreases with the radius of the collector.

Drag Force

The drag force acting on a particle can be described as (Watson, 1973)

$$\mathbf{F}_{\mathrm{d}} = 6\pi\eta b\left[\bar{\mathbf{i}}_{\mathrm{r}}\left(V_{\mathrm{r}} - V_{\mathrm{pr}}\right) + \bar{\mathbf{i}}_{\theta}\left(V_{\theta} - V_{\mathrm{p}\theta}\right)\right] \tag{2}$$

where η is the fluid dynamic viscosity. This equation includes the particle velocity, V_{pr} and $V_{\mathrm{p}\theta}$, and the fluid velocity, V_{r} and V_{θ}, in the radial and tangential directions. The components of fluid velocity for laminar flow are given by (Batchelor, 1970):

$$V_r = -V_0 \frac{\ln\left(\frac{r}{a}\right) - 0.5\left[1 - \left(\frac{a}{r}\right)^2\right]}{2.002 - \ln \Re} \sin\left(\theta - \gamma\right) \tag{3a}$$

$$V_{\theta} = -V_0 \frac{\ln\left(\frac{r}{a}\right) + 0.5\left[1 - \left(\frac{a}{r}\right)^2\right]}{2.002 - \ln \Re} \cos\left(\theta - \gamma\right) \tag{3b}$$

where $\Re$ ($= 2V_0\rho_f a/\eta$) is the Reynolds number and V_o is the magnitude of the fluid velocity.

These equations show that the drag force should increase with particle size, fluid viscosity, and fluid velocity, and decrease with wire radius.

Gravitational Force

The gravitational force ($\mathbf{F}_g$) can be described as (Svoboda, 1987)

$$\mathbf{F}_g = \frac{4\pi b^3}{3}(\rho_p - \rho_f)g\left[\bar{\mathbf{i}}_r \cos(\theta - \beta) - \bar{\mathbf{i}}_\theta \sin(\theta - \beta)\right] \tag{4}$$

where g is the gravitational acceleration and ρ_p and ρ_f are the particle and fluid densities, respectively. This equation shows that the gravitational force increases with particle size and density and decreases with fluid density.

Incorporating these three forces into a force balance is the basis for the trajectory model (Watson, 1973):

$$\mathbf{F}_g + \mathbf{F}_m + \mathbf{F}_d = 0 \tag{5}$$

The solution to this equation yields a differential equation which describes the path of the particle, i.e. how R varies as a function of □ with respect to the wire collector. Thus, this equation is properly called the "trajectory equation" (Ying, 2000):

$$\frac{dR}{d\theta} = R\frac{G\cos(\theta - \beta) - \frac{V_m}{a}\left(\frac{M}{2H_0}\frac{1}{R^5} + \frac{\cos 2\theta}{R^3}\right) + \frac{V_r}{a}}{G\sin(\theta - \beta) + \frac{V_m}{a}\frac{\sin 2\theta}{R^3} + \frac{V_\theta}{a}} \tag{6}$$

where

$$G = \frac{2b^2\left(\rho_p - \rho_f\right)}{9\eta a}g$$

$$V_m = \frac{2b^2\mu_0\chi_p MH_0}{9\eta a}$$

The trajectory equation can be solved by numerical methods to determine the limiting trajectory (Payatakes, 1973; Vaidyanathan, 1986; Tien, 1989). The limiting trajectory represents the "watershed path" of the particle that separates the paths that lead to the collector, and thus result in capture, from paths that lead away from the collector, and thus result in escape (Figure 2). From this specific path, one can derive a critical radius, R_c, which is defined as the distance between the starting point of the limiting trajectory and the axis that passes through the center of the wire collector (Figure 2).

The critical radius is the key parameter for the prediction of the removal efficiency. From it, one can determine total capture cross-sectional area per unit length of wire and the number of particles that will be removed per a differential thickness of the filter. Integrating over the entire length of the filter, one can estimate the number of particles removed from the filter, and thus the overall removal efficiency. This procedure, developed by Watson (1973), relates RE to R_c by the equation:

$$\text{Removal efficiency } (RE) = 1 - C_{out}/C_{in} = 1 - \exp\left[\frac{-4(1-\varepsilon)LR_c}{3\pi a}\right] \qquad (7)$$

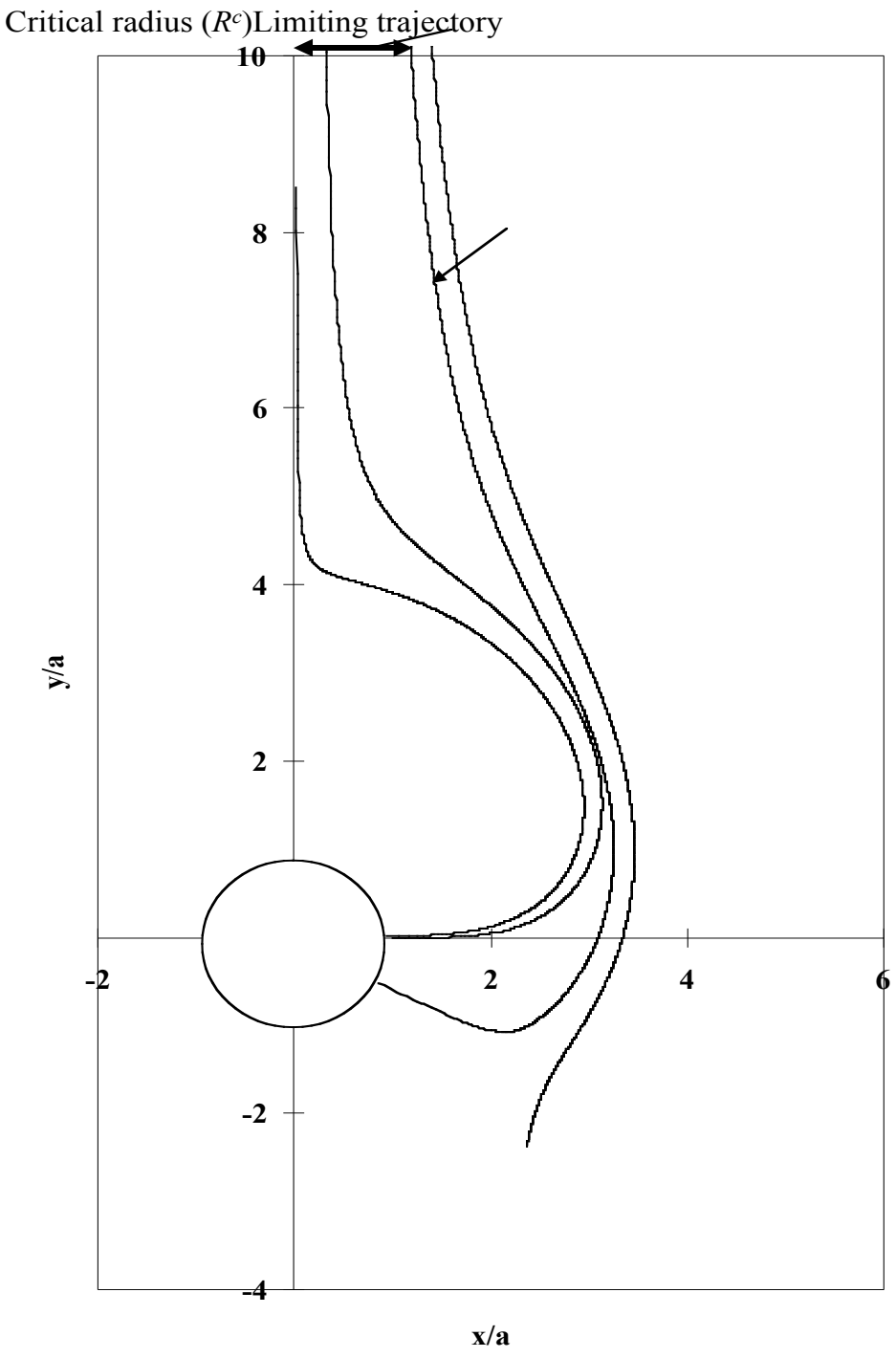

Figure 2: Illustration of the limiting trajectory and critical radius for small paramagnetic particles captured by a wire. Coordinates are normalized to *a*, the radius of the collector (Ying 2000).

where L represents the length of the filter and $1-\varepsilon$ the packing density of the filter medium.

A second criterion for evaluating the performance of a filter is its longevity. Because filters become fouled, they must be cleaned, or regenerated, periodically. A filter must be regenerated when the effluent concentration of the contaminant exceeds a specified threshold level, above which the concentration is unacceptable. This condition is known as filter breakthrough. Since filter regeneration necessarily interrupts the process, it is costly in terms of time and money. Therefore, a filter should be designed to reduce the frequency of regeneration.

A model that could predict the time it takes for a filter to reach breakthrough would be very useful for the design of magnetic filtration systems. The trajectory model is valid only for a clean filter because it does not account for the accumulation of particles on the filter medium, it is not valid over the entire filtration cycle, which includes particle build-up and breakthrough. Furthermore, since there is no time component in the trajectory model, an additional model is necessary to predict how long a filter will last until breakthrough. The longevity of a filter is closely related to its capacity for retaining particles. A filter's retention capacity is called its "loading volume." The amount of particles a filter can capture is finite. When the volume of particles captured by the filter exceeds the loading volume, additional particles will escape capture and exit the filter, thus increasing the contaminant concentration in the effluent. If one could predict the loading volume of a filter, and the time it takes to reach

this capacity based on the rate of particle removal, then it would be possible to predict when the effluent concentration will exceed breakthrough.

Such a "breakthrough model" was developed by Ying (2000). Based on the trajectory model described above, a particle build-up model that predicts the total particle loading volume and a bivariate population-balance (PB) model (Tsouris et al., 1995) that calculates the size and magnetic susceptibility distribution of polydispersed particles, this model produces a "breakthrough curve" that predicts how the effluent particle concentration changes with time. How are these three models used in the breakthrough model? The bivariate PB model predicts a range of particle size classes. From the trajectory model, the RE is calculated for each particle size class; and from the build-up model, the loading volume is likewise calculated for each class. The time component is introduced to the model through a particle volume flow rate, J_k, which is also different for each particle class. The particle removal rate for each class is equal to the product of J_k and RE_k. Dividing the loading volume (from the buildup model) for the first class size, which is the smallest, by the sum of J_k x RE_k for all classes, one can calculate the breakthrough time for the first class. Similarly, a characteristic breakthrough time can be calculated for each size class, except that the loading volume of the previous classes must be subtracted from the loading volume of the next class and the particle removal rate for the previous classes must be excluded from the summation of J_k x RE_k. The result is a distinct breakthrough time for each class. Coupled with the calculation of the particle

volumetric flow rate for each class in the effluent, an effluent concentration versus time graph can be estimated.

2.2 Non-Magnetic Filtration Mechanism

For a particle to be retained by a filter and removed from the fluid, two things must happen: 1) the particle must collide with the filter medium; and 2) the particle must be deposited onto the filter medium. Thus, the filtration process consists of two steps: transport and attachment. In magnetic filtration, the transport and attachment to the filter medium depend solely on the magnetic force. In non-magnetic filtration, three classic mechanisms have been used to describe particle transport to the filter medium: sedimentation, interception, and diffusion. Sedimentation occurs when the density of the particle exceeds the density of water, and so its movement is influenced by the gravitational force. Interception occurs when the particle is large enough to collide with the collector as it moves along with the flow of the fluid. Diffusion is a result of the Brownian motion of the particle due to random collisions with molecules in the fluid.

Trajectory theory can also be used to model these transport mechanisms. By predicting the path of the particle through the filter media, the ratio of the number of actual collisions to the number of potential collisions between the particle and collector can be estimated (the 'collector efficiency', □). Fundamental models have been developed to predict the contribution of each of these transport mechanisms to collision efficiency (Yao, Habibian, and O'Melia, 1971):

$$\eta_G = \frac{(\rho_p - \rho_f)gb^2}{18\mu V_o} \tag{8}$$

$$\eta_I = \left(\frac{3}{2}\right)\left(\frac{b}{d}\right)^2 \tag{9}$$

$$\eta_D = 0.9\left(\frac{kT}{\mu b d V_o}\right)^{2/3} \tag{10}$$

$$\eta = \eta_G + \eta_I + \eta_D \tag{11}$$

where d is the diameter of a spherical filter grain. The overall collector efficiency, □, is the sum of the efficiency of each transport mechanism.

According to these models, the collector efficiency, □, is a function of various parameters: particle density and diameter, collector diameter, flow velocity, temperature, and viscosity. These equations predict generally that the efficiency of a filtration process will be lowered by higher flow rates, smaller particles (unless they are small enough that diffusive transport is significant), and larger collector diameters.

It is important to note that these models only describe the transport step of filtration. If the particles collide with the collectors, but do not adhere, then they will not be removed. Thus, to model filtration effectively, it is also necessary to predict what fraction of these collisions will result in capture. A second term, the collision efficiency factor (□), is used to describe how many collisions result in actual particle capture. The collision efficiency factor depends on the particle stability, and so it is determined by the short-range forces between particles and between particles and collectors. These forces include van der Waals and electrostatic forces, and may also include non-DLVO forces such as steric, hydration, and hydrophobic/hydrophilic forces. The general principle is that the stronger the attractive forces are relative to the repulsive forces, the higher the

collision efficiency. If the particles are completely destabilized, □ = 1, the trajectory models can be used directly to determine the efficiency of a filter. Otherwise, the collision efficiency must be also accounted for to predict the efficiency. The ratio of effluent to influent concentration, which is used to calculate RE, is given by Equation 12 (Yao, Habibian, and O'Melia, 1971):

$$\ln\left(\frac{C}{C_o}\right) = -\frac{3}{2}(1-\varepsilon)\alpha\eta\left(\frac{L}{d}\right) \tag{12}$$

According to these models, the bigger and 'stickier' a particle is, the easier it is to remove by filtration. Thus, filtration processes in water treatment are typically preceded by a coagulation step in which chemicals are added to destabilize the particles so that they aggregate. However, when the treatment goal is to not only remove particles from water, but also to separate them from other particles in order to recover and reuse them, it may be desirable to add chemicals that can stabilize particles to prevent aggregation and lower the removal efficiency.

2.3 Surfactants

Surfactants are one class of chemicals that can be used to stabilize particles in aqueous suspensions. Surfactants can adsorb onto the surface of particles. Adsorbed surfactants can stabilize the particles by increasing the electrostatic repulsion, by adding steric repulsion, or by altering the hydophobicity of the particle surface. The effectiveness of a surfactant at stabilizing particles depends on the concentration of surfactant at the interface (the adsorption density), the packing and orientation of surfactant molecules at the interface, and the charges on the molecules (Somasundaran, 1997).

These factors in turn depend on the physical (surface area, porosity, etc.) and chemical characteristics of the surface; the chemical characteristics of the surfactant (chain length, branching, functional groups); the interactions between the surfactant and solvent (solubility, micellization); the characteristics of the solvent (polarity, pH, ionic strength); and the interactions between the surfactant and the surface (Somasundaran, 1997). Ionic surfactants charged oppositely of the particle surface will make the surface more hydrophobic since the charged hydrophilic head group will be attracted to the surface, orienting the hydrophobic tail away from the surface into the solvent. Conversely, ionic surfactants with the same charge as the surface will make the surface more hydrophilic, if the hydrophobic tail is attracted to the surface. The charged head group, oriented into the solvent, may also increase the surface charge of the particle, making it more stable electrostatically. The longer the protruding chain, the stronger the steric force.

By altering the surface properties of the particles, surfactants can affect the filtration of particles by non-magnetic mechanisms. Surfactant adsorption can make particles smaller by limiting aggregation. Smaller particles generally have lower collector efficiencies, and are thus harder to remove by filtration. Surfactant adsorption can increase the repulsive forces between the particles and collectors. Stronger repulsive forces, relative to attractive forces, lower the collision efficiency, making filtration less effective.

CHAPTER 3

MATERIALS AND METHODS

Filtration experiments were conducted with Ferric Oxide (Fe_2O_3) particles (EM Science, Gibbstown, NJ) and 430 stainless steel wool pads (Aquafine Corporation.). The experimental apparatus consisted of five main components (Figure 3): 1) a water-jacketed feed tank; 2) a Branson 2210 ultrasonic cleaner (Branson Ultrasonic, Danbury, CT); 3) a peristaltic pump (Rainin Instrument Co., Inc., Oakland, CA); 4) a bipolar electromagnet (Applied Magnetic Laboratory, Baltimore, MD); and 5) a magnetic filter. Under continuous sonication (to prevent aggregation and maintain a uniform particle size), the feed was pumped to the magnetic filter, across which a magnetic field was applied. Effluent samples were collected at periodic time intervals throughout the duration of the experiment. After particles from these samples were digested in trace-metal grade hydrochloric acid (Fisher Scientific), iron concentration was measured using atomic absorption spectroscopy (AAS).

The feed was composed of Fe_2O_3 particles (500 ppm) suspended in deionized water. The ionic strength was adjusted to 0.001 N by adding NaCl. To increase particle stability and help prevent aggregation, the pH was raised to 9.5 – 10.0 by adding NaOH (0.1 N). In the surfactant-treatment experiments, 10 mM of sodium dodecyl sulfate (SDS), cetyl trimethyl ammonium bromide (CTAB), or Tween 80 was added to the feed.

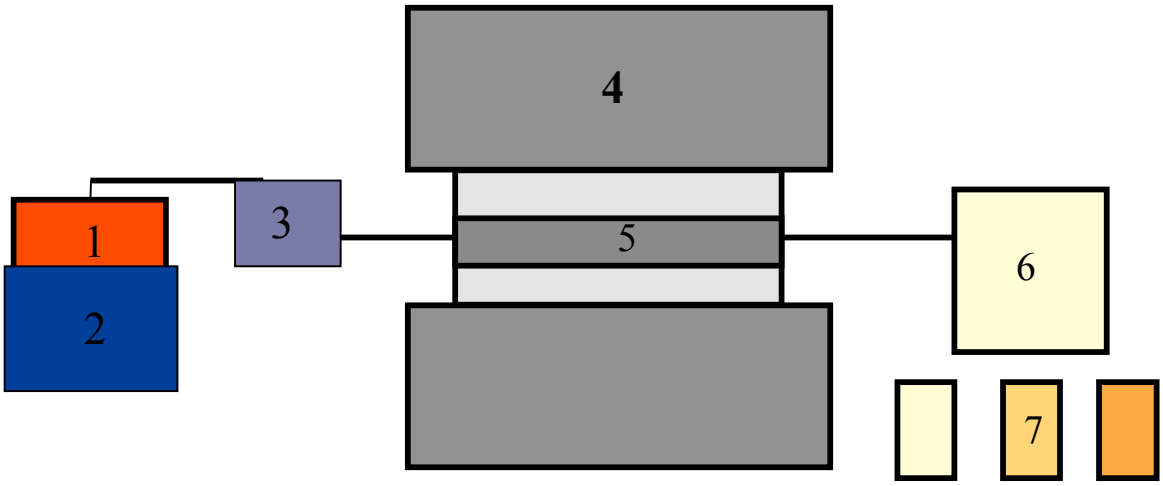

Figure 3: Schematic of magnetic filtration experimental set-up (1 – water-jacketed feed tank; 2 – ultrasound cleaner; 3 – peristaltic pump; 4 – electromagnet; 5 – steel wool filter; 6 – effluent tank; 7 – effluent samples).

Before each run, the feed was pre-mixed by 30 minutes of sonication. To keep the feed temperature from rising, cool faucet water was circulated continuously through the water jacket. This method held the feed temperature between 26 and 30^{o}C.

To achieve a packing density of 4.4%, 1.36 g of steel wool was randomly and uniformly packed into a glass cylinder (1 cm ID) and compressed to a length of 5 cm. The same packing density was used for each experiment. Random, uniform packing was achieved by pulling apart the steel wool fibers and carefully inserting small amounts at a time into the glass cylinder. The steel wool filter was mounted in an aluminum spacer (0.75 in. thickness), which was secured between the two poles of the electromagnet.

Before each run, the filter was wetted with 20 mL of a surfactant solution (SDS, 10mM), and then rinsed with 100 mL of water. The purpose of this step was to help ensure that the feed flowed uniformly through the column and thus made contact with all

of the steel wool by displacing the air in the column and removing residual oil from the surface of the wool.

The magnetic field strength delivered by the bipolar electromagnet was controlled by a Precision Bipolar Magnet Controller (Applied Magnetic Laboratory Inc., Baltimore, MD). The applied magnetic field strength was set by adjusting the electric current on the controller. The level of current was determined by an empirical correlation between current, field strength, and spacer thickness, provided by the manufacturer. The magnetic field was turned on five minutes after the beginning of each experiment.

Effluent samples were collected at periodic intervals, the length of which depended on the total run time. From each sample, a volume of 1 or 2 mL aliquot was added to 3 mL of HCl, and left to sit overnight. The acid dissolved completely the solid particles, leaving free iron in the solution. The concentration of iron was measured with an AAanalyst 800 Atomic Absorption Spectrometer (Perkin-Elmer, Norwalk, CT). From these iron concentration measurements, the Fe_2O_3 concentration in the effluent was deduced.

After running the feed through the filter for 120-180 minutes, the pump was stopped and the filtration column was removed from the electromagnet and mounted vertically. The liquid in the column was drained into a beaker, and a sample was collected for AAS analysis. Then the glass tube portion of the column, containing the steel wool, was filled with water and immersed in the ultrasound cleaner. After sonicating for 1 minute, the liquid was drained into a beaker, and a sample was collected for AAS analysis.

The particle size distribution was measured by a Brinkman 2010 Particle Size Analyzer (Brinkman Co., Westbury, NY), which detects particles over the range of 0.5 to 150 μm. For these measurements, a few drops of feed sample were collected from the pump outlet in a water-filled cuvette. The measurement was taken immediately after it was collected. Additional measurements were obtained from a dynamic light-scattering device, which measures particle size in the range of 1 nm to 1μm. An inversion routine attached to the instrument estimates the particle size distribution.

The design parameters tested were applied magnetic induction, fluid velocity, and wire diameter. The effect of the magnetic field strength was tested at 0.2 and 0.5 T; the effect of fluid velocity was tested at 0.1, 0.3, and 0.5 cm/s; and the effect of wire diameter was tested for ultrafine, medium, and course grade steel wool (average diameters were 37, 72, and 98 μm, respectively). These parameters were studied with and without SDS treatment.

CHAPTER 4

RESULTS AND DISCUSSION

4.1 Modeling Results and Analysis

4.1.1 Trajectory Model

Using the trajectory eqn (6) and eqn. (7), one can predict the effect of the design parameters on the removal efficiency of a clean filter. The trajectory equation was solved by an algorithm developed for the *Engineering Equation Solver* software (Ying, personal communication). The model input and output parameters are summarized in Table 1. The wire radius, superficial velocity, and applied magnetic induction are design factors. The range of values selected for the model paralleled the range tested experimentally. The other input parameters are non-design factors that were controlled experimentally. The saturation magnetization, filter length, and filter porosity are characteristics of the filter medium. The volume magnetic susceptibility, the particle density, and particle radius are characteristics of the ferric oxide particles. The choice of 0.5 μm for the particle radius is based on particle size distribution measurements from two sources (see experimental results below) and represents a mean value since the particles were polydispersed. The fluid density and dynamic viscosity are characteristics of the fluid medium; the values are for pure water at 25^{o}C. The model results are displayed in Figures 4-9.

Table 1: Input and output parameters for the trajectory model

Inputs	Symbol	Level(s)	Outputs
Wire radius (microns)	a	10 – 60	Critical Radius, Rc (dimensionless)
Superficial velocity (m/s)	V_o	0.001 - 0.007	
Applied magnetic induction (T)	B_o	0 - 0.8	
Saturation magnetization (T)	M_s	0.6	
Filter length (m)	L	0.05	
Filter porosity (dimensionless)	ε	0.956	Removal Efficiency, RE (dimensionless)
Particle radius (microns)	b	0.5	
Volume magnetic susceptibility (dimensionless)	χ_p	0.000480	
Particle density (kg/m^3)	ρ_p	5240	
Fluid density (kg/m^3)	ρ_f	997	
Dynamic viscosity (kg/m-s)	η	0.001	

Figures 4-7 show the model response to the factors that affect the magnitude of the magnetic force. The values for the three variables that were used in the calculations are reported for each figure; the values for all other parameters fixed at the levels reported in Table 1. As the magnitude of this force increases, the RE improves sharply. According to Equation 1, the magnetic force increases with the magnetic field strength, particle size, and magnetic susceptibility, and decreases with the collector radius. That

these parameters have a similar effect on the RE indicates that the magnetic force is the primary cause of particle capture.[1]

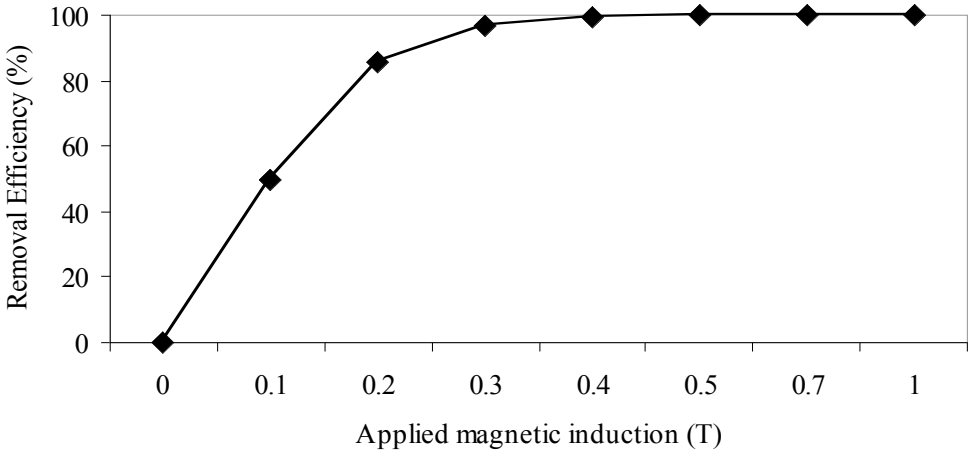

Figure 4: Response of the trajectory model to applied magnetic induction, B_o. (a = 15 µm; V_o = 0.003 m/s)

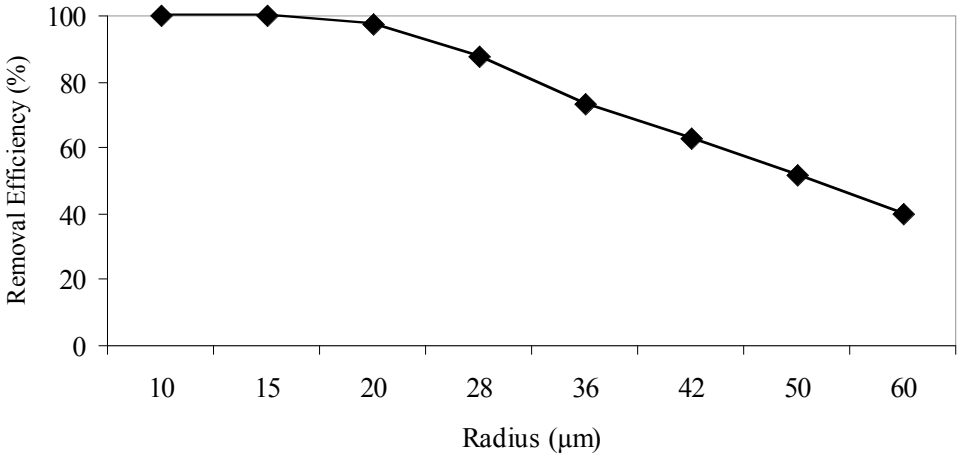

Figure 5: Response of the trajectory model to wire radius, a. (B_o = 0.2 T; V_o = 0.003 m/s).

[1] Though both the magnetic force and drag force increase with particle size, the increase of the magnetic force is on the order of b^3, while the increase of the drag force is on the order of b, which is why RE increases with b.

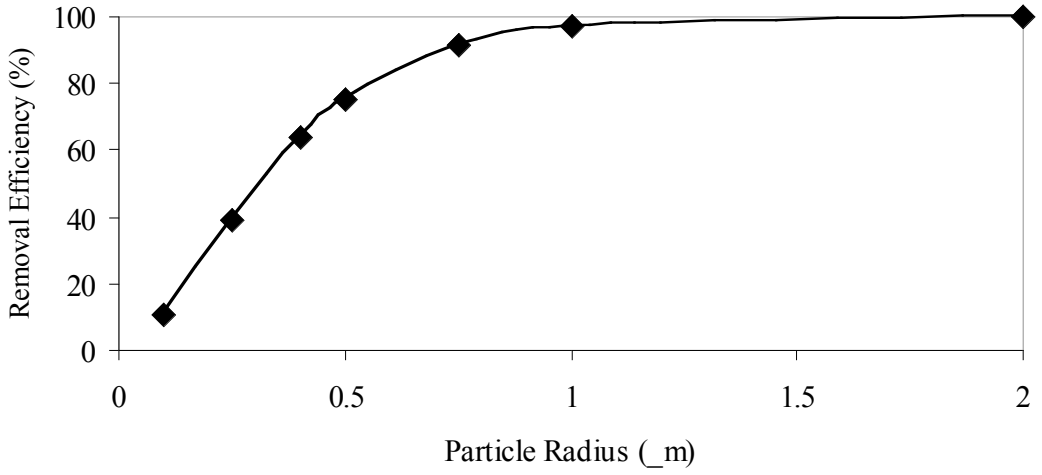

Figure 6: Response of trajectory model to particle radius, *b*.
(a = 30 μm; B_o = 0.2 T; V_o = 0.003 m/s).

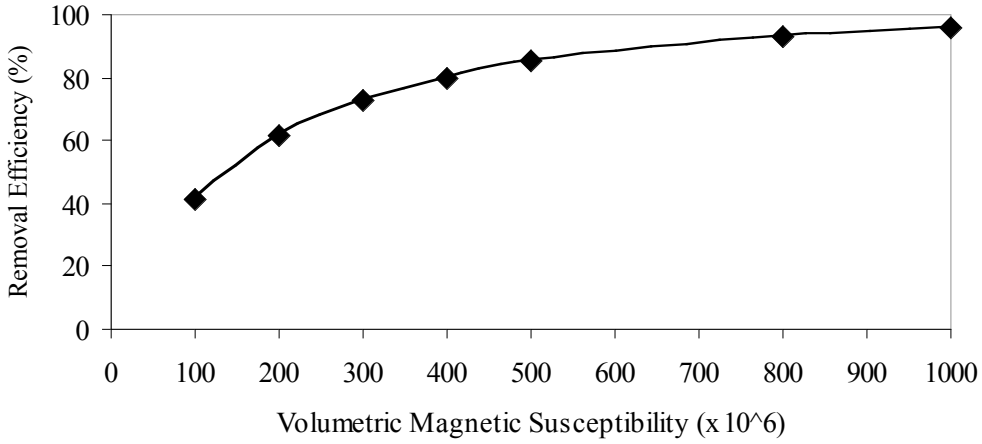

Figure 7: Response of trajectory model to magnetic susceptibility of the particle, □$_p$.
(a = 15 μm; B_o = 0.2 T; V_o = 0.003 m/s).

Figures 8-9 show the model response to the factors that affect the magnitude of the drag force. According to Equation 2, the drag force increases with fluid velocity and viscosity. The model predicts that as the magnitude of this force increases, the RE decreases. Thus, the drag force counters the magnetic force to prevent particle capture.

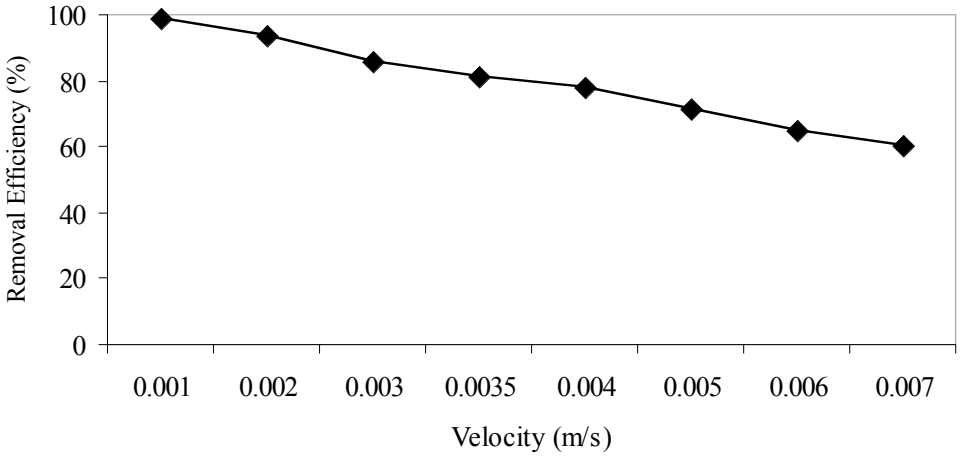

Figure 8: Response of the trajectory model to fluid velocity, V_o (B_o = 0.2 T; a = 15 μm).

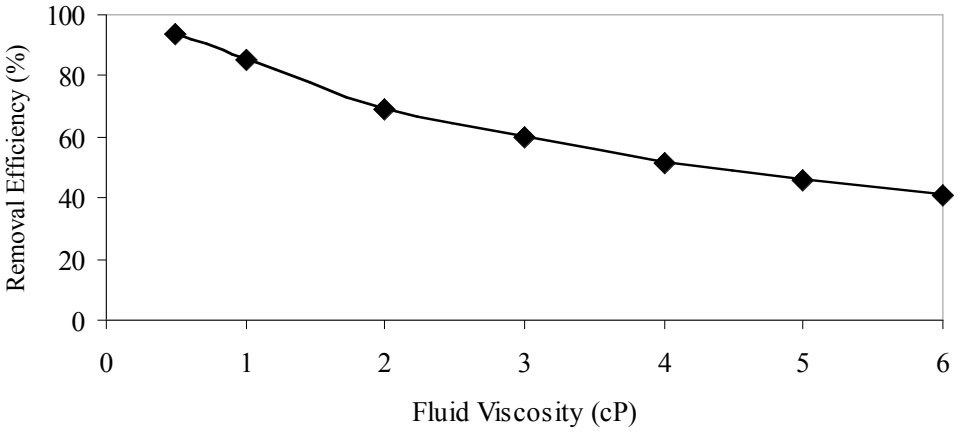

Figure 9: Response of trajectory model to fluid viscosity, □. (a = 15 μm; B_o = 0.2 T; V_o = 0.003 m/s).

These model predictions demonstrate that the magnetic filtration mechanism operates by a competition between two basic forces: the magnetic force works to capture particles while the drag force works to prevent particles from capture. This interpretation is supported by three simple observations. First, when the applied magnetic field strength is zero, the removal efficiency is also zero. The reason for this outcome is that in the model only the magnetic force influences the trajectory of the particle towards the wire collector. Second, the factors that strengthen the magnitude of the magnetic force – field strength and wire diameter - improve filter performance. This force is proportional to the applied magnetic field strength and inversely proportional to the wire thickness. Consequently, as the former increases and as the latter decreases, the removal efficiency increases. Third, the removal efficiency decreases with an increase in velocity. The intensity of the drag force is directly proportional to the fluid velocity. Thus, as the velocity increases, so does the drag force. Under a stronger drag force, the particles are more likely to escape capture and be carried away by the flow of the bulk fluid. The removal efficiency is higher at lower velocities because the magnetic force faces less competition from the drag force for particle capture.

According to these results, the model should predict well the effect of these parameters on the RE of a filtration process in which the magnetic force is the primary mechanism for particle capture, dominating other attractive forces, and in which the drag force dominates other repulsive forces. However, if there are other mechanisms at work in the process which the model does not incorporate, then the model predictions will deviate from experimental results. If the removal of Fe_2O_3 particles from water is due to a magnetic mechanism, then we should expect to see a similar response from the filter to

these three parameters in the experimental data. However, if the experimental RE of the filter responds oppositely to the model, or if the performance of the filter is unresponsive to these parameters, then non-magnetic mechanisms are responsible for particle removal and should be incorporated in the model.

4.2 Experimental Results and Analysis

4.2.1. Filtration Experiments with Fe_2O_3 and Water

The results of filtration experiments with Fe_2O_3 particles and water are displayed in Table 2. These results demonstrate that mechanisms other than the magnetic mechanism are primarily responsible for particle capture. Two observations support this claim. First, attractive forces other than the magnetic force are capturing the majority of the particles. When Bo = 0 T, there is no magnetic force. Nonetheless, over 90% of the particles were removed. Clearly, there are other forces involved in this process. Second, the parameters that change the magnetic force have no statistically significant effect on the performance of the filter.[2] As Table 2 shows, RE only increases from 90 to 98% when the field strength is increased from 0 to 0.5 T; and there is virtually no change in

Table 2: Response of the filter to the three design parameters. The baseline parameters were $B_o = 0.2$ T; $V_o = 0.3$ cm/s; and a = 15 μm, except $B_o = 0.5$ T for the wire radius factor.

Design Parameter	**Level**	**RE (experimental)**
Applied Magnetic Induction (B_o)	0 T	90.1 +/- 9.9%
	0.2 T	96.6 +/- 11.0 %
	0.5 T	98.1 +/- 11.0%
Wire Radius (a)	49 μm	89.1 +/- 9.8%
	36 μm	91.9+/- 10.1%
	15 μm	98.1 +/- 11.0%
Fluid Velocity (V_o)	0.5 cm/s	94.2 +/- 10.4%
	0.3 cm/s	96.6 +/- 11.0 %
	0.1 cm/s	100%

[2] This result is a consequence of the high RE at 0 T. With only 10% of the particles 'available' for removal by the magnetic mechanism, it is difficult to see the effects of these parameters.

RE when the field strength is increased from 0.2 to 0.5 T. The response of the filter to changes in fluid velocity and wire diameter is similar: from 0.5 to 0.1 cm/s, the RE increases from 94 to 100%; and from 49 to 15 μm, the RE increases from 89 to 96%. However, none of these variations in RE is outside of the range of experimental error. The performance of HGMS has been shown to depend largely on a competition between the magnetic and drag forces (Ying, 2000). This process, though, is essentially unresponsive to the factors that determine the strength of these two forces. Second, the majority of the particles are removed without a magnetic field.

Traditional filtration theory (Chapter 2) helps us explain why the filter removed over 90% of the particles by non-magnetic mechanisms. First, if the Fe_2O_3 particles aggregate, the particle size is larger, and the collector efficiency should increase due to the transport mechanisms of interception and sedimentation. Second, because the particles adhere readily to surfaces, i.e., they are very sticky, they should have a high collision efficiency.

We tried to prevent aggregation by applying ultrasonic waves to the feed, which broke-up aggregates, and by raising the pH of the feed to 9.5. Zeta potential measurements suggest that in this pH range, the particles are negatively charged, and should be stable (Figure 10). These zeta potential data are consistent with the measured effect of pH on the particle size distribution (Figure 11). Figure 11 shows that, as the pH increases, the percentage of particles below 1 micron diameter increases while the maximum particle diameter decreases, signifying that less aggregation occurs.

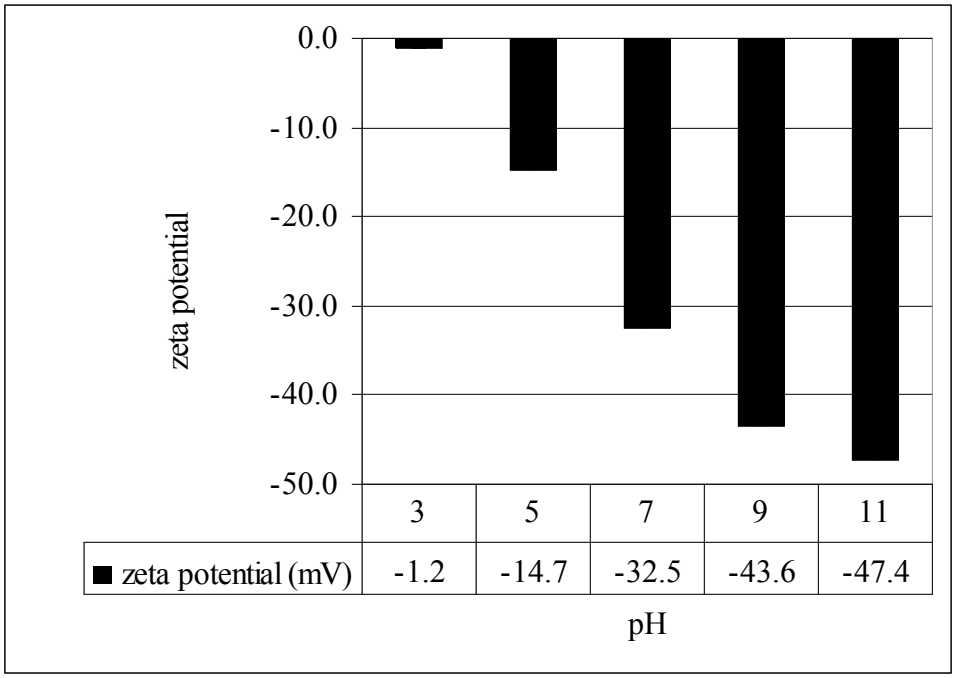

Figure 10: Effect of pH on particle stability, as measured by zeta potential.

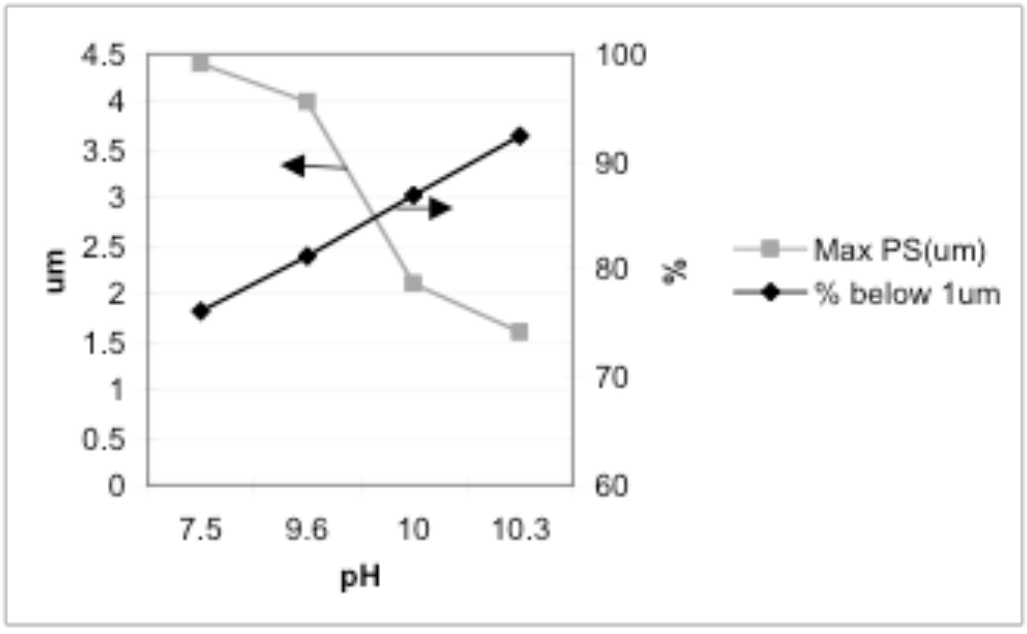

Figure 11: Effect of pH on PSD of Fe_2O_3 particles.

Despite our efforts to prevent aggregation, we have reasons to believe that some aggregation still occurred. One reason is that the PSD changed as the feed was transported from the feed tank to the filter. The mean particle diameter in the feed collected from the tank was 0.69 +/- 0.18 μm, with only 6% of particles greater than 1 μm, and with a maximum particle diameter of 1.6 μm. The mean particle diameter collected from the outlet of pump was 0.90 +/- 0.61 μm, with over 25% of particles greater than 1 μm, and with a maximum particle diameter over 10 μm. These data indicate that some aggregation occurs in the pump tubing. If measurable aggregation occurred in the small volume of the pump tubing over a short time period, then it is reasonable to infer that there was also aggregation in the column below the filter medium – a much larger volume with a longer residence time. This conclusion is consistent with the color of the suspension in this region of the column – a brick-red color characteristic of large aggregates, as distinct from the orange-red color characteristic of finer particles in suspension. A second reason is that the pH of the feed tended to decrease over time (Figure 12). Since particle stability is affected by pH, aggregation might have increased with time also. Figure 12 shows the effect of this pH drift on the PSD.

We did not quantify the effects of aggregation on collector efficiency. However, we did observe a significant amount of sedimentation. After every experiment a noticeable amount of particles were deposited on the bottom of the filter, which was placed horizontally in the magnetic field. This further supports the claim that particle aggregation was a factor in filtration.

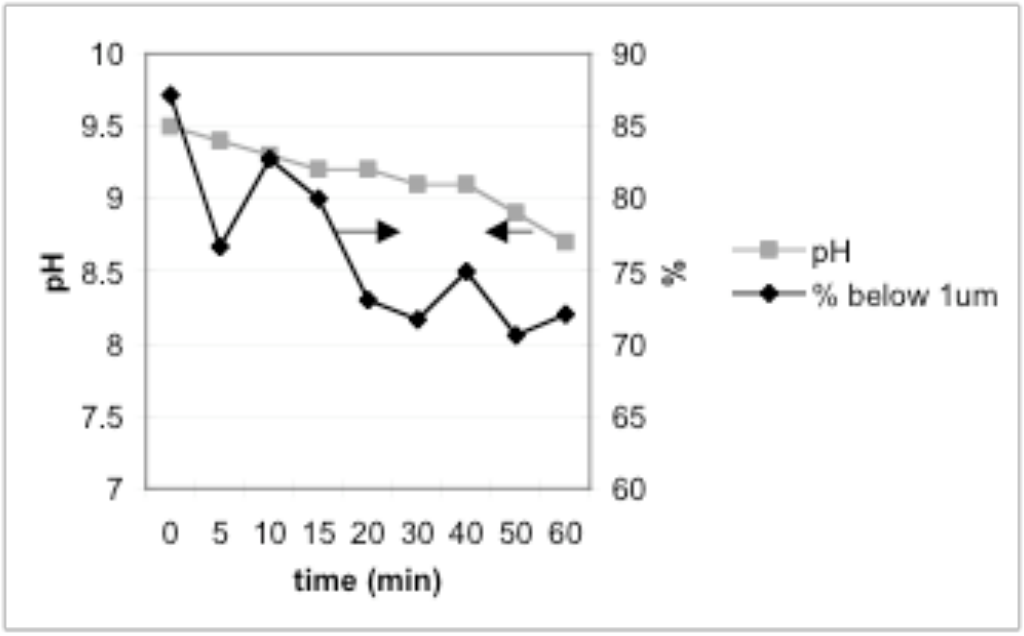

Figure 12: Effect of pH drift over time on PSD of Fe_2O_3 particles.

The second aspect of non-magnetic filtration to consider is the collision efficiency. The Fe_2O_3 particles adhere to all kinds of different surfaces. With a bright red-orange color, the particles leave a distinct mark on every surface with which they come in contact. The particle suspensions leave a red-orange residue on glassware and on the Teflon tubing used in the experimental apparatus. This residue is not easy to remove: vigorous washing with a brush and soap, or ultrasound cleaning is required. Consequently, the experimental apparatus may retain as high as 20% of the particles (Figure 13). That the particles also adhere strongly to the surface of the steel wool is shown by the difficulty of regenerating the filter after an experiment. Even after flushing the filter with water under ultrasonic waves, particles remained firmly attached to the filter surface.

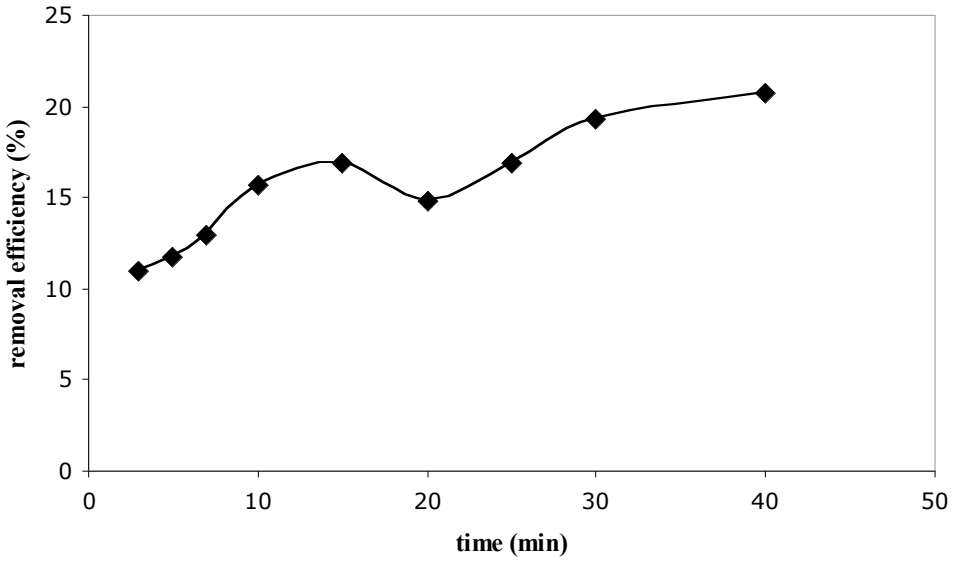

Figure 13: Removal of Fe_2O_3 particles with no filter medium.

Why are Fe_2O_3 particles so strongly attracted to the surface of stainless steel? What forces account for this attraction? These forces are strong enough to resist the effect of the drag force over the range the fluid velocity that was tested experimentally. The fluid velocity had an insignificant effect on the RE (Table 2), indicating that the drag force was not strong enough to overcome the attractive force between the particles and collector. These forces are strong enough to overcome the electrostatic repulsion between the particle and the steel. The zeta potential of stainless steel at pH 10 (□ = -37.2) demonstrates that that the surface was negatively charged. An attractive van der Waals force exists between the particles and steel wool, but this force is not strong enough to account for this effect.

What appears to be happening in this process, then, is that the particles are colliding with the wire collectors via sedimentation and interception, and they are sticky enough that the majority of these collisions are successful. The bottom line is that large,

sticky aggregates are easy to remove, even in a very porous filter like the one we used. Therefore, to reduce the impact of the non-magnetic mechanism on the removal of particles, it is necessary to both minimize aggregation and to make the particles less adherent to the steel wool surface. This was attempted by treating the feed suspension with SDS.

4.2.2. Filtration Experiments with Fe_2O_3, SDS, and Water

Results of filtration experiments with Fe_2O_3, SDS, and water are displayed in Table 3. These results demonstrate that when the feed is treated with SDS, particle

Table 3: Response of filter performance to design parameters for SDS-treated Fe_2O_3 particles.

Design Parameter	**Level**	**RE (experimental)**
Applied Magnetic Induction (B_o)	0 T	10.8 +/- 0.8 %
	0.2 T	79.9 +/- 6.5 %
	0.5 T	93.4 +/- 7.5%
Wire Radius (a)	49 μm	60.2 +/- 4.8%
	36 μm	71.4 +/- 5.7 %
	15 μm	93.4 +/- 7.5 %
Fluid Velocity (V_o)	0.5 cm/s	69.5 +/- 5.6%
	0.3 cm/s	78.4 +/- 6.3 %
	0.1 cm/s	95.3 +/- 7.6%

capture is due primarily to the magnetic mechanism. Two observations support this claim. First, the majority of the particles are captured by the magnetic force. In contrast to the 90% removal with no SDS by non-magnetic mechanisms, only 10% of the particles were removed at 0 T. Second, the design parameters have a significant effect on the RE (Table 3). An increase in applied magnetic induction from 0.2 to 0.5 T increased the RE

from 79.9 to 93.4%; an increase of fluid velocity from 0.1 to 0.5 cm/s decreased the RE from 95.3 to 69.5%; and a decrease of wire radius from 49 to 15 μm increased the RE from 60.2 to 93.4%.

When the magnetic force is strengthened by increasing the applied magnetic induction or by decreasing the average wire diameter, the filter removes more particles. When the drag force is strengthened by increasing the fluid velocity, the filter removes fewer particles. Thus, these results capture the competition between the magnetic force and drag force over particle capture. This competition is the essence of the magnetic filtration mechanism.

The effect of these parameters on RE is more pronounced because SDS-treatment minimizes the influence of non-magnetic mechanisms on particle capture. SDS weakens these mechanisms by making the particles more stable and less sticky.

Changes in aggregation behavior demonstrate the effect of SDS on particle stability. Left undisturbed in a beaker of water, SDS-treated particles settle at a much slower rate than non-treated particles, signifying lower aggregation. Particle size distribution (PSD) data explain this behavior and confirm that SDS treatment reduces particle aggregation. Table 4 shows the effect of SDS treatment on four parameters related to aggregation: average particle diameter, average standard deviation (S.D.) of each particle size measurement, the largest particle size measured, and the percentage of particles with a diameter below 1 micron. The mean particle diameter and % below 1 μm data show that SDS-treatment causes a smaller particle size. More noteworthy, though, are the mean S.D. and maximum particle diameter. That the mean S.D. is nearly four times less for SDS-treated particles indicates a more uniform suspension. This

conclusion is also supported by the maximum particle diameter data. The largest particle in an SDS-treated suspension is an order of magnitude smaller than the largest particle in an untreated suspension.

Table 4: The effect of SDS-treatment on particle stability **(**10 mM SDS; all samples taken from pump outlet**)**

SDS treatment	Mean diameter (μm)	Mean SD (μm)	Mean maximum diameter (μm)	% below 1μm
Yes	0.67	0.16	1.3	97.6
No	0.90	0.61	11.9	77.9

This effect of SDS on particle stability is corroborated further by PSD measurements from a second instrument that uses dynamic light scattering. The advantage of this instrument is that its range is smaller than 0.5 microns. Therefore, it could detect the full breadth of the size distribution. Measurements from this instrument are displayed in Figure 14. Figure 14 shows that SDS-treatment, coupled with ultrasonic treatment to break-up aggregates, creates a relatively homogenous size distribution, indicating that SDS has a stabilizing effect on the particles.[3]

[3] Note that the mean radius of 0.24 microns differs from the mean radius of 0.34 microns measured by the other instrument. The former was used in the model because of the range limitations of the first instrument. In the first instrument, the mode fraction was 0.55 microns. That the mode was lower than the mean suggests the existence of particle sizes below the instrument range. In the second instrument, the median and mean are essentially equal, suggesting that the instrument range covered the range of particle sizes.

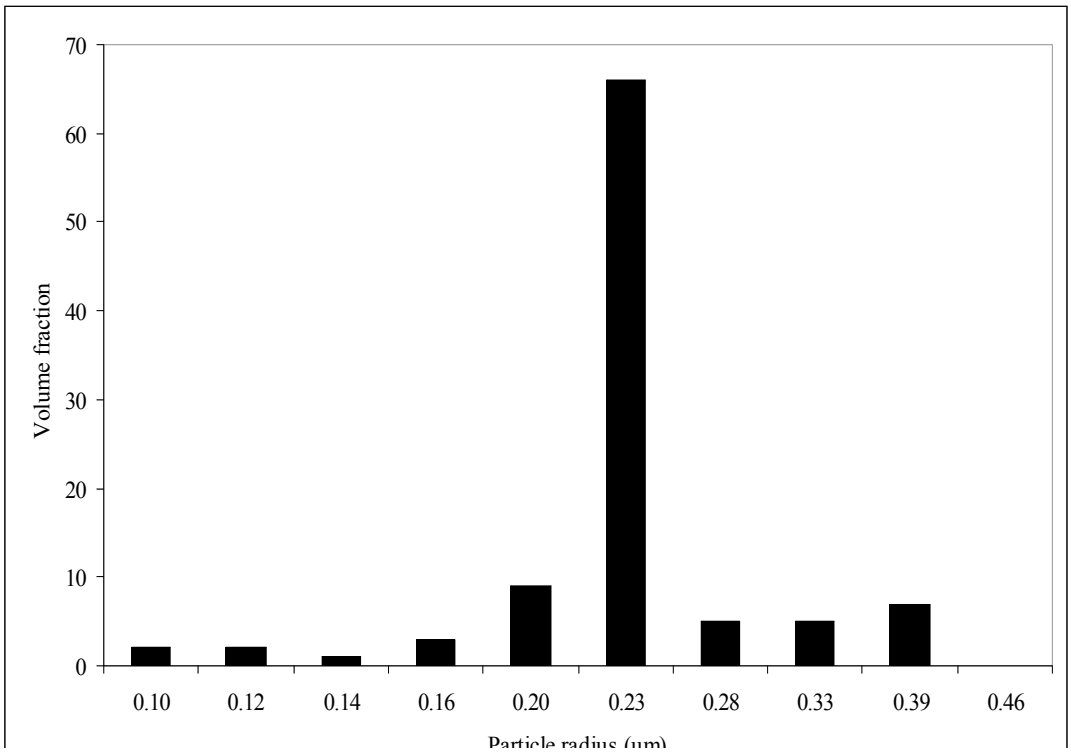

Figure 14: PSD of SDS-treated ferric oxide (mean b = 0.24 μm; relative variation = 0.060)

The stabilizing effect of SDS is demonstrated also by how the RE of the filter changes with respect to time. Figure 15 shows that with SDS treatment, the RE decreases sharply with time. For each experiment with SDS-treated particles under these conditions, the RE decreased by 10-11% over 20 minutes. The RE decreases quickly because as particles are deposited on the wire, inter-particle repulsion thwarts capture of additional particles on those sites. In contrast, with SDS-free particles, RE is more stable over time, indicating that captured particles do not inhibit additional particle capture. For each experiment with SDS-free particles under the same conditions, the RE remained essentially constant over 20 minutes (Figure 16). As these particles are deposited on the wire, inter-particle attraction could facilitate the capture of additional particles.

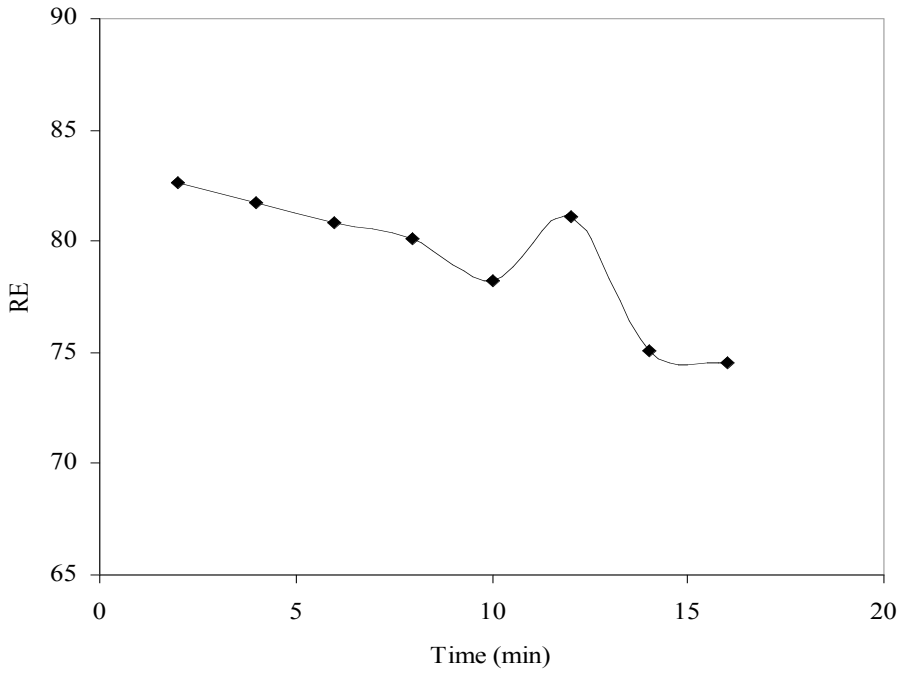

Figure 15: Effect of SDS-treated Fe_2O_3 particle build-up on RE

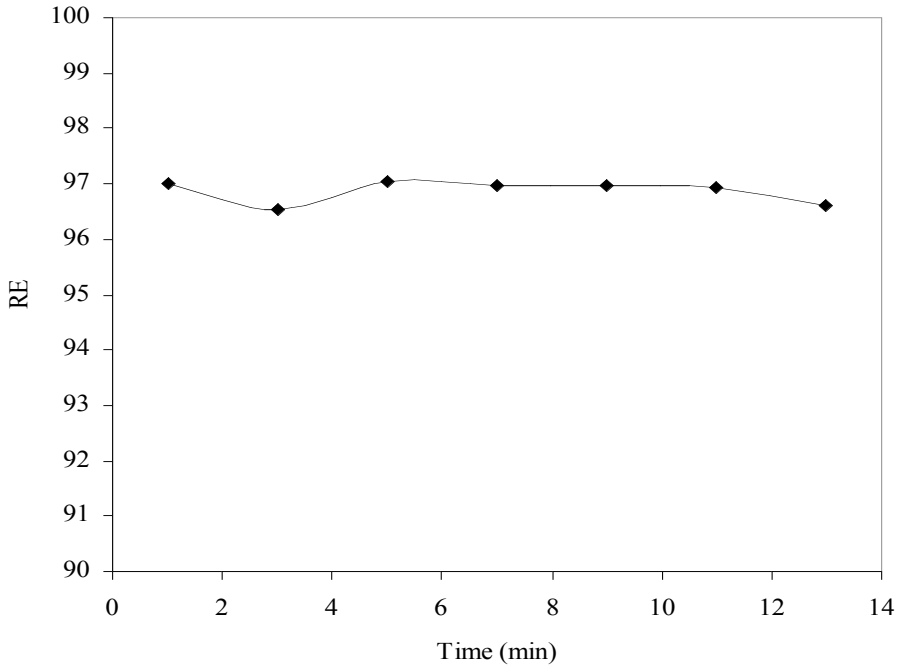

Figure 16: Constancy of RE over time for SDS-free Fe_2O_3 particles (B_o = 0.2 T; V_o = 14 mL/min; a = 14.5 um).

This evidence indicates that SDS treatment enhances particle stability and thus limits particle aggregation by increasing repulsive forces between particles. How does SDS strengthen the inter-particle repulsive force, and so enhance particle stability? Two classic mechanisms for particle stability are electrostatic stabilization and steric stabilization. Electrostatic stabilization arises from a repulsive force created by the interaction of the electrical double layers of the particle surfaces. Steric stabilization arises from surfactant or polymer adsorption at solid-water interfaces. Electostatic stabilization can be assessed quantitatively by measuring the zeta potential of a particle, but steric stabilization is very difficult to quantify. Since SDS is an anionic surfactant, we might expect that adsorption on the particle surface would increase the overall negative charge on the surface, and thus stabilize the particle electrostatically. If greater electrostatic stabilization occurs, one would expect SDS treatment to increase the zeta potential of the particles. Figure 17 compares zeta potential measurements for particles with and without SDS.

Since the zeta potential measurements are essentially the same, it is likely that SDS treatment does not stabilize the particles via electrostatic stabilization. This result and conclusion disagrees with the work of Ma and Li (1990) who show that the zeta potential of Fe_2O_3 increases with SDS concentration, and thus attribute the stabilizing effect of SDS to electrostatic repulsion. The results may differ because our experiments were run at a pH of 10, where the zeta potential was high enough already that SDS adsorption would not increase significantly the net surface charge. This explanation agrees with Ma and Li's observation that the change in zeta potential plateaus above the

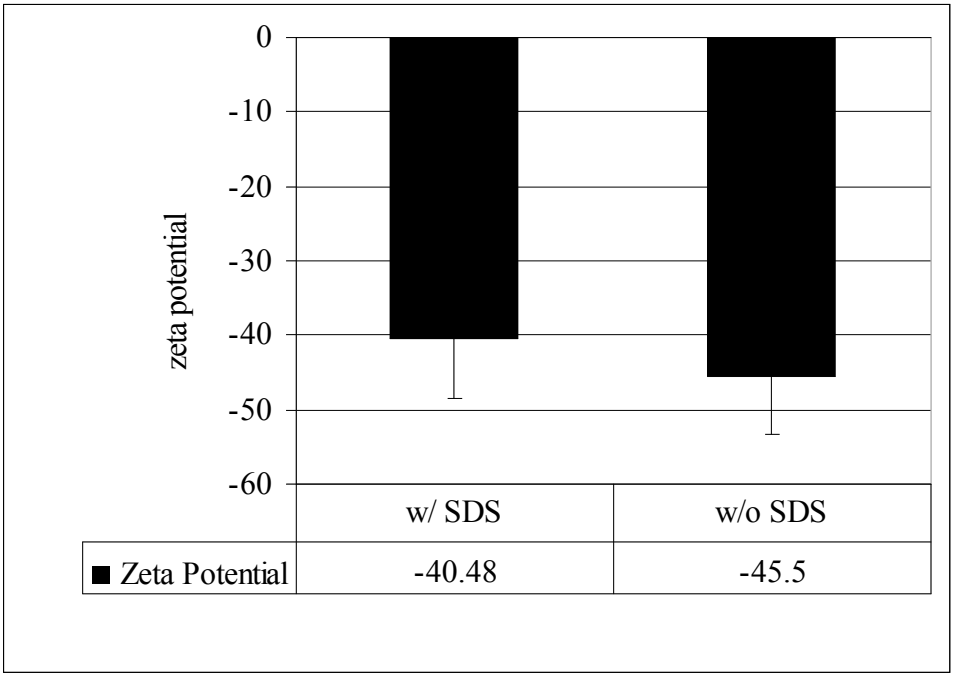

Figure 17: Effect of SDS on zeta potential of Fe_2O_3 particles.

critical micelle concentration (CMC) of SDS. Furthermore, the concentration of SDS used in our experiments exceeded the CMC of SDS. In the region of the CMC, the Fe_2O_3 particles are close to being saturated with the surfactant. Therefore, much of the SDS was not adsorbed, but was in the bulk solution. In this situation, we might expect SDS treatment to have the opposite effect because adding SDS to the feed solution significantly increases the ionic strength. At [SDS] = 10 mM, the ionic strength is 0.010 N – ten times that of the SDS-free suspension (I = 0.001 N). This increase in ionic strength is verified by conductivity measurements of both solutions. The conductivity of SDS-free solutions was approximately 180 μS/cm, compared to 730μS/cm for SDS-treated solutions. By increasing the ionic strength of the solution, SDS could potentially compress the electrical double-layer around the particles, and so reduce the zeta potential.

The other possible mechanism of particle stability is steric stabilization. Steric barriers are formed when adsorbed molecules protrude into the solvent and interact with each other. The steric effect depends on the density of adsorbed chains, and on the length of the chains (Rosen, 1989). This force is repulsive because when two particles with adsorbed molecules move towards each other, the entropy per adsorbed molecule decreases, which increases the interfacial energy, and thus requires work to bring the particles closer (Somasundaran, 1997).

By stabilizing the Fe_2O_3 particles, the SDS reduces the contribution of the sedimentation and interception transport mechanisms to the collector efficiency, and so may also decrease the number of particle-collector collisions.

SDS also makes the particles less adherent to surfaces. Two observations support this claim. First, when particles are treated with SDS, they do not leave behind an orange-red residue on the surface of the glass feed tank or the Teflon tubing. Second, it is much easier to regenerate filters that contain SDS-treated particles. Samples of the fluid from the filtration column were collected after filtration experiments were performed with and without SDS, using the same parameters, and the Fe_2O_3 concentration was measured. With SDS, the mass of Fe_2O_3 in the filter fluid was 514 mg, representing 89% of the total mass of Fe_2O_3 captured by the filter. Without SDS, the mass of Fe_2O_3 was 138 mg, representing just 31% of the total mass captured (Figure 18). Samples were collected and measured again after sonicating each column for one minute.

Previous research on the effect of SDS adsorption on the agglomeration and breakup of magnetic particles sheds light on why surfactant treatment results in superior recovery of particles (Chin, Yiacoumi, and Tsouris, 2003). SDS adsorption onto

superparamagnetic particles was shown to cause reversible secondary minimum aggregation in the presence of a magnetic field. This was demonstrated experimentally by the break-up of particles after the field was removed. Similarly, in this process, SDS adsorption creates a secondary minimum potential energy between a Fe_2O_3 particle and steel wool collector, and between agglomerated particles on the steel wool surface. Consequently, the particles break-up and are readily removed when the field is removed from the filter.

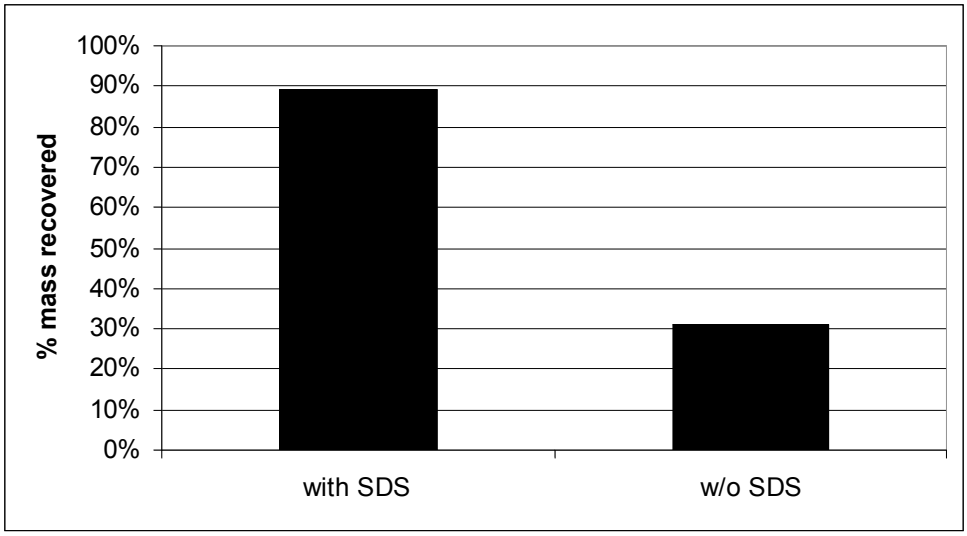

Figure 18: The effect of SDS on the recovery of Fe_2O_3 from the filter after disabling the magnetic field.

By stabilizing the particles and making them adhere weakly to surfaces, SDS adsorption lowers both the collector and the collision efficiency of the filter, and so essentially eliminates the impact of the non-magnetic mechanism on the overall removal efficiency of this process.

4.2.3 Filtration Experiments with Fe_2O_3 and Cationic and Nonionic Surfactants

Figure 19 compares the RE of Fe_2O_3 particles treated with CTAB and Tween 80 versus SDS for both non-magnetic and magnetic filtration. Though RE due to the magnetic mechanism is essentially the same, there is a noticeable difference in non-magnetic RE. These results suggest that the CTAB creates a slightly stronger steric repulsion between the particle and collector surfaces, while Tween 80 creates a weaker steric repulsion. There are two possible explanations for why CTAB adsorption causes stronger steric force. First, as a cationic surfactant, CTAB should adsorb more efficiently

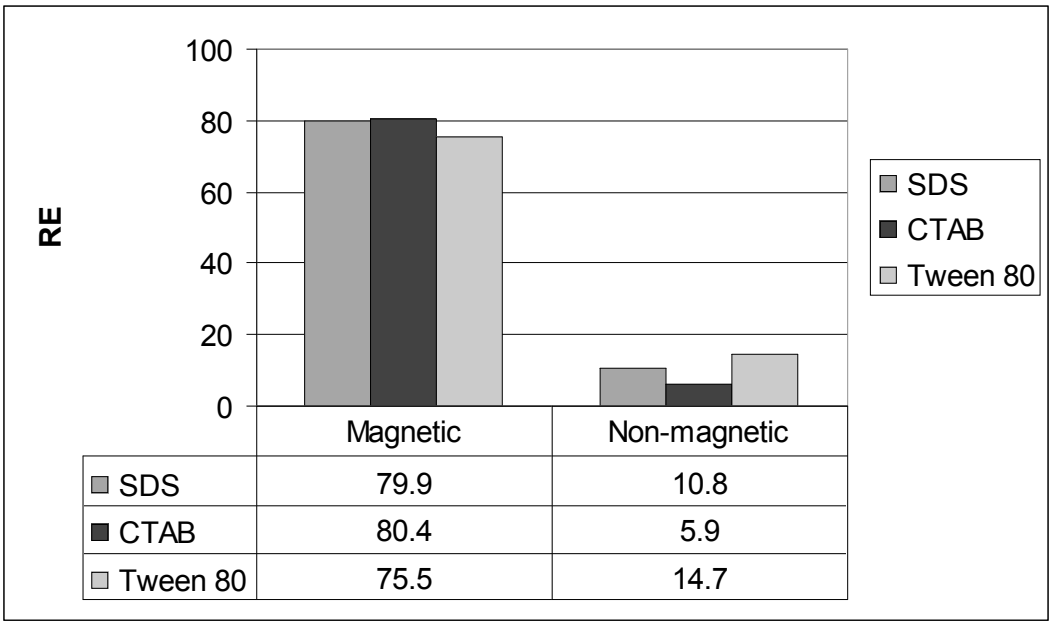

	Magnetic	Non-magnetic
SDS	79.9	10.8
CTAB	80.4	5.9
Tween 80	75.5	14.7

Figure 19: Comparison of the Effect of Various Surfactant Types on RE.

to the negatively charged Fe_2O_3 surface. Thus, the adsorption density of CTAB molecules should be higher. Second, CTAB, with 19 carbon molecules in its hydrophobic chain, is

a longer molecule than SDS, which has 12 carbon molecules in its chain. The strength of the steric force is related directly to the protrusion length of the adsorbed molecule (Israelachvili, 1992). The difference in the repulsive force, however, is not great enough to overcome the attractive magnetic force. Hence, the particles are removed via the magnetic mechanism at the same rate, regardless of the type of surfactant added.

4.2.4 Filtration Breakthrough Experiments

The effect of applied magnetic induction and SDS treatment on filter breakthrough were also tested in this study. The results are displayed in Figures 20 and 21. Cout* represents the effluent concentration normalized to the feed concentration. Figure 20 shows that the applied magnetic induction not only improves the RE of the filter in the beginning stage of filtration, but it also increases the loading capacity of the filter, a parameter that is germane to the overall filter performance because it determines how often the filter must be regenerated. At 0.2 T, the magnetic force is not strong enough to overcome the inter-particle repulsive forces created by electrostatic and steric interactions. Consequently, the rate of particle capture decreases sharply as particles build up on the surface of the collectors. However, at 0.8 T, the magnetic force remains strong enough to dominate these forces even as more particles are deposited on the surface. Consequently, the rate of particle capture remains steadier throughout the course of the experiment.

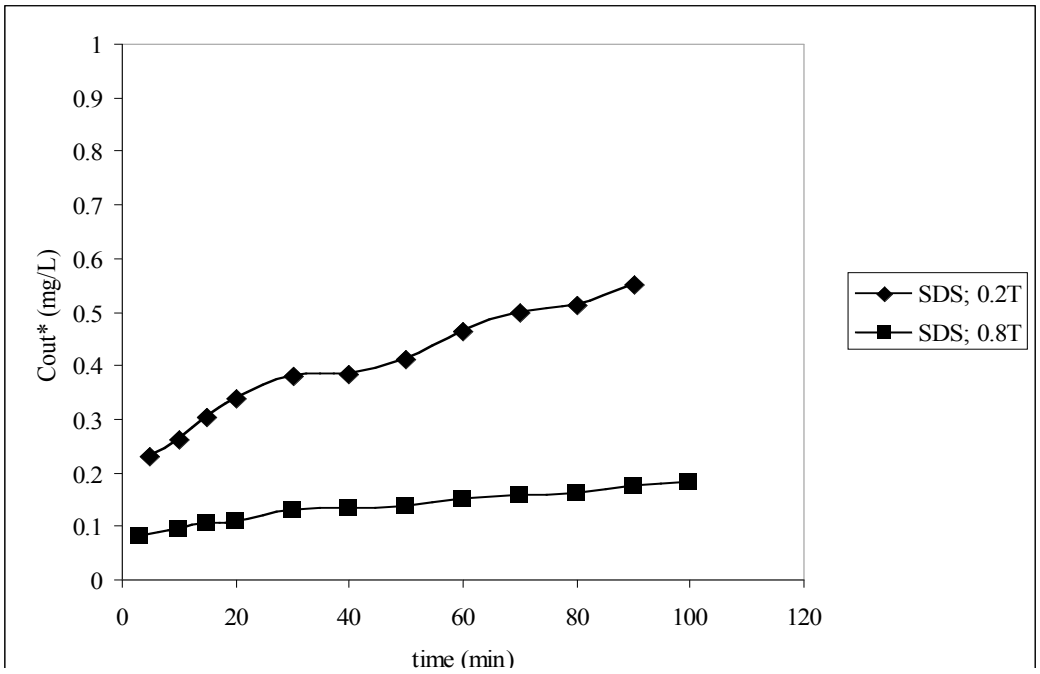

Figure 20: Effect of applied magnetic induction on filter breakthrough (V_o = 0.003 cm/s; a = 15 μm).

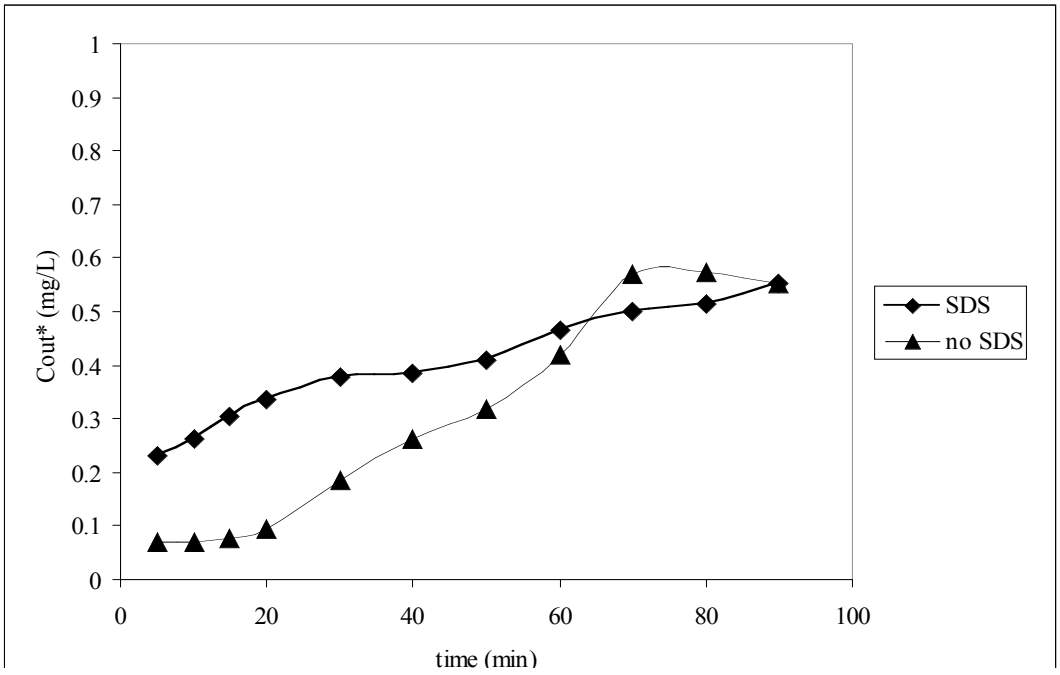

Figure 21: Effect of SDS-treatment on filter breakthrough (B_o = 0.2 T; V_o = 0.003 cm/s; a = 15 µm).

4.3 Comparison between Modeling and Experimental Results

4.3.1 Modeling Results verses Experimental Results for Fe_2O_3 particles with no SDS

Results from experiments without SDS differ sharply from the modeling predictions. The experimental results show essentially no response to the parameters, but the modeling results predict that the RE is very sensitive to these parameters. The model predicts an increase in RE from 85.5 to 99.9% in response to an increase in B_o from 0.2 to 0.5 T; an increase in RE from 71.1% to 99.0% in response to a decrease in V_o from 0.5 cm/s to 0.1 cm/s; and an increase in RE from 52.0 to 99.9% in response to a decrease in a from 49 to 15 μm.

The model is much more responsive to these parameters because it assumes that the magnetic mechanism is not only the dominant, but the sole mechanism of filtration. In the model, no other force besides the magnetic force contributes to particle capture. Thus, when $B_o = 0$, RE equals zero. However, as reported above, this was not the case experimentally. The steel wool filter consistently achieved a RE of over 90% in the absence of a magnetic field.

The success of a trajectory analysis depends on the inclusion and accurate expression of the relevant forces into the model (Tien, 1989). Therefore, the model predictions might be more accurate if additional forces were incorporated into the model. The experimental results show that other major forces are involved in the transport and deposition of particles onto the collectors. Adding these forces to the model might show that conventional filtration mechanisms are stronger than magnetic filtration mechanisms in the case that particles form large aggregates.

Herein lies the reason why the response of the filter to these parameters is so low. Because non-magnetic mechanism achieves such a high RE, only a small fraction of the particles are affected by the magnetic mechanism. Thus, the effect of the magnetic-drag force competition is obscured. However, if one excludes this 90% of particles not removed by magnetic filtration from the feed concentration used to calculate RE, the experimental results reveal a heightened sensitivity to these parameters. For example, with this modification a change in fluid velocity from 0.5 to 0.1 cm/s results in an increase in RE from 47 to 97%. Likewise, a change in magnetic induction from 0.2 to 0.5 T results in an increase in RE from 75 to 90%. This analysis suggests that if the non-magnetic mechanisms could be dismantled experimentally, then the magnetic mechanism in this process could be studied more carefully.

4.3.2. Modeling Results verses Experimental Results for Fe_2O_3 particles with SDS

The modeling results show a much closer agreement with the experiments with SDS. Figures 22-24 compare the response of the model and the experimental system to changes in the design parameters. This comparison shows that the model and experiments with SDS respond similarly to these factors.

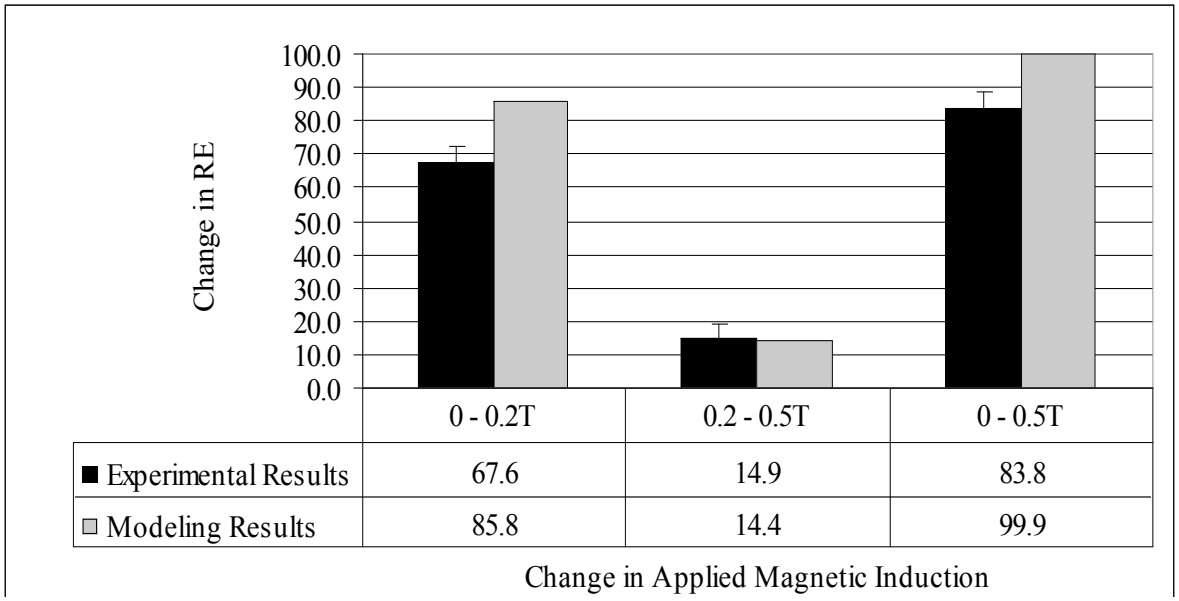

Figure 22: Comparison of the model and experimental response to changes in the applied magnetic induction (B_o) for the removal of SDS-treated Fe_2O_3 particles (b = 0.25 μm).

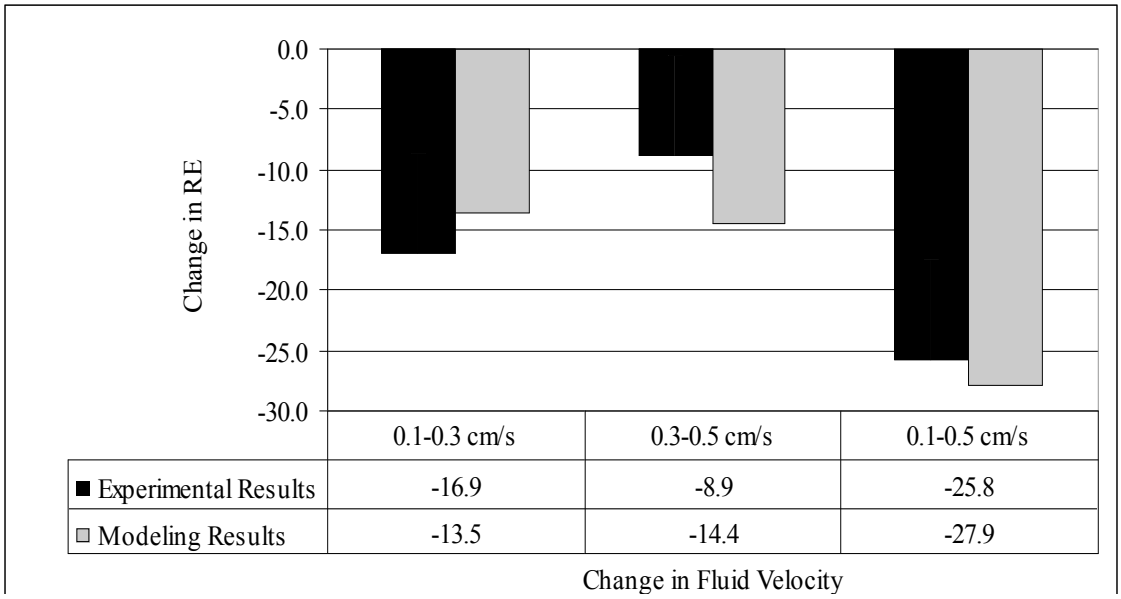

Figure 23: Comparison of the model and experimental response to changes in the fluid velocity (V_o) for the removal of SDS-treated Fe_2O_3 particles (b = 0.25 μm).

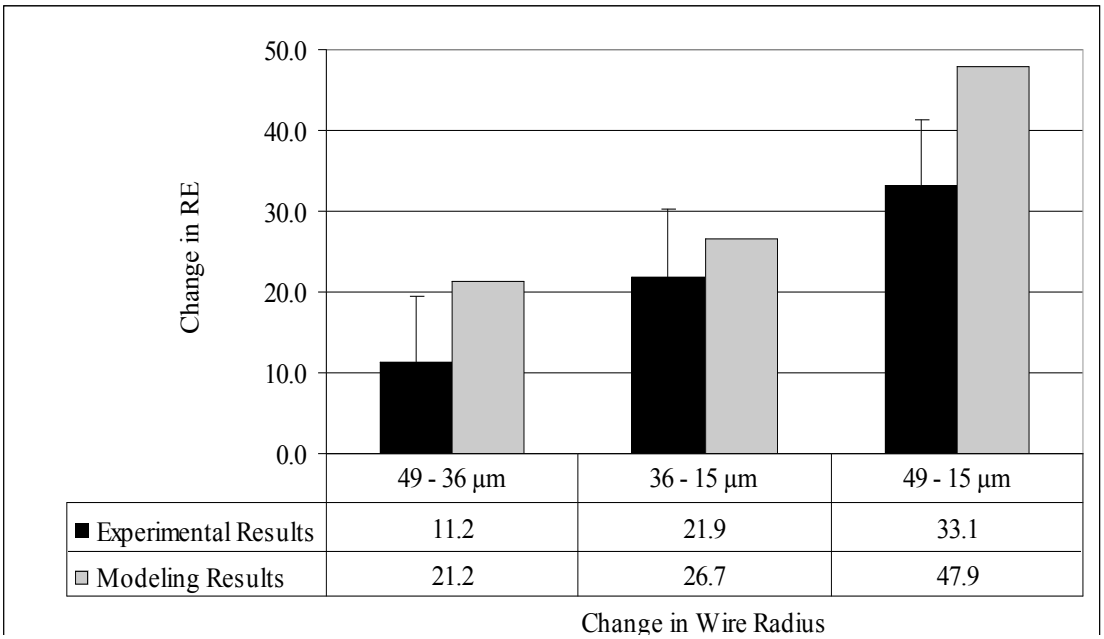

Figure 24: Comparison of the model and experimental response to changes in the average wire diameter ($d = 2a$) for the removal of SDS-treated Fe_2O_3 (b = 0.25 µm).

An absolute comparison of the effect of these parameters on RE also shows a good agreement between modeling and experimental results. Figures 25-27 show that not only does the model predict well the experimental trends, but at each level of all three parameters the RE predicted by the model lies within the experimental error of the corresponding experimental RE.

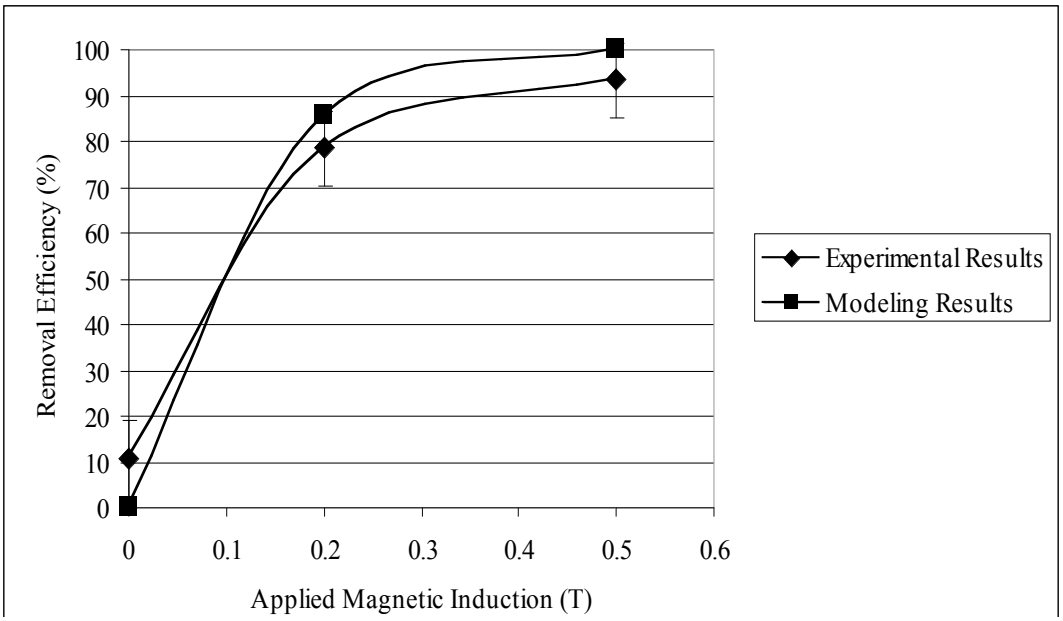

Figure 25: Comparison of the predictions of the trajectory model with experimental results for the effect of applied magnetic induction on the removal of SDS-Treated Fe_2O_3 Particles (b = 0.25 μm).

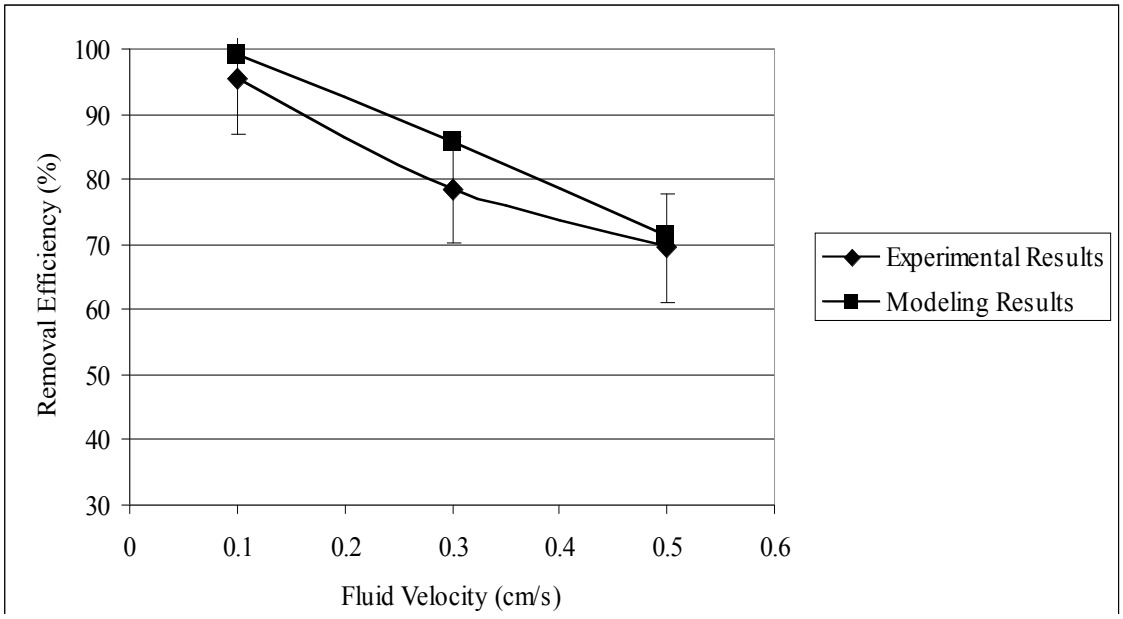

Figure 26: Comparison of the predictions of the trajectory model with experimental results for the effect of fluid velocity on the removal of SDS-treated Fe_2O_3 particles (b = 0.25 μm).

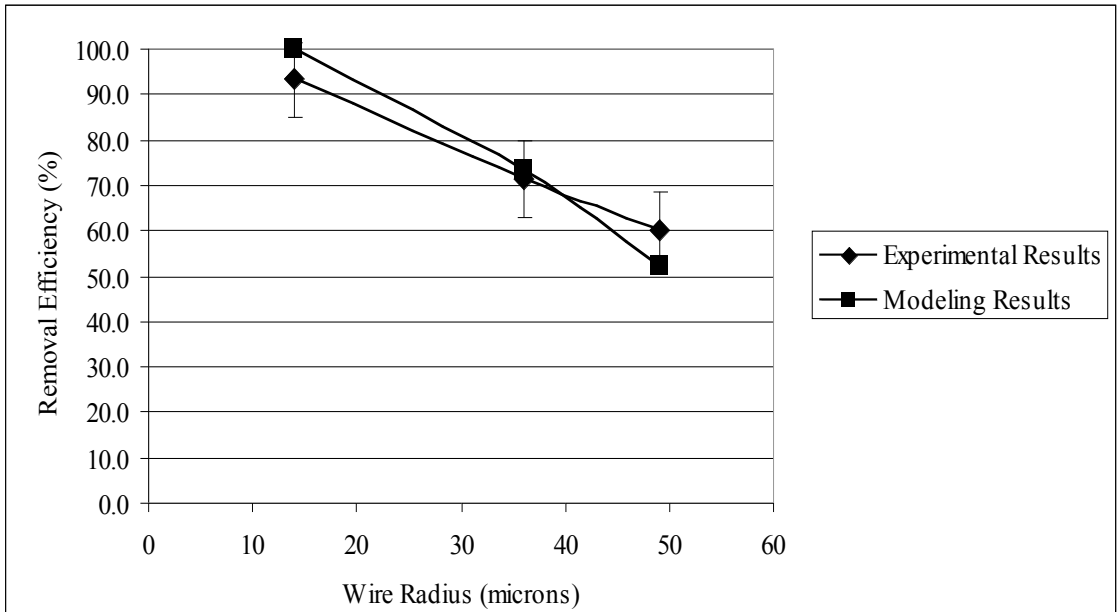

Figure 27: Comparison of the predictions of the trajectory model with experimental results for the effect of wire radius on the removal of SDS-treated Fe_2O_3 particles (b = 0.25 μm).

That these experimental results closely parallel the trends predicted by the trajectory model further substantiates the claim that the removal of SDS-treated particles is due primarily to the operation of the magnetic mechanism If the experimental filtration mechanism corresponds to the filtration mechanism simulated by the model, then the sensitivity of the experimental process and the model to changes in the design parameters should be similar. Figures 22-24 compare the impact of changes in the levels of the three design parameters on experimental and modeling results. Figure 22 shows a remarkable consistency between model and experimental sensitivity to an increase in B_o from 0.2 to 0.5 T. The somewhat greater sensitivity of the model over the range of 0 to 0.2 T can be explained by the approximately 10% removal of particles due to non-magnetic filtration. Thus, in the experimental system, magnetic filtration is the dominant, but not the sole

mechanism for particle removal. Figure 23 shows a close similarity between the model and experimental sensitivity to the fluid velocity, V_o. The model again predicts a remarkably similar response to a change in this parameter from 0.5 to 0.1 cm/s. These similarities can be explained by the fact that the model simulates accurately the interaction between the magnetic force and drag force that determines particle capture.

It is noteworthy that the trajectory model works well, even though it does not consider the repulsive forces between the particle and collector caused by electrostatic and steric interactions. Though these forces are pertinent to removal by a non-magnetic mechanism, because they are dwarfed by the magnetic force, they present negligible opposition to capture by the magnetic force.

4.4 Significance of Results

These findings have important implications for the use of HGMS to remove paramagnetic particles from water, or from a suspension of a mixture of particles. First, if the particles targeted for removal have similar properties to ferric oxide particles with respect to aggregation and their attraction to surfaces, then HGMS may not be the best technique for separating the particles. If 90% RE is achieved by a filter with such a high porosity (96.5%), then non-magnetic filters with a lower porosity, like granular filters, would perform even better. These filters would demand less operating costs than a HGMS process because there would be no energy required to generate a magnetic field.

Second, HGMS could be useful for separating paramagnetic particles via magnetic filtration from diamagnetic particles (particles with very low or negative magnetic susceptibility). To achieve this separation, it would be necessary to minimize

the impact of non-magnetic filtration mechanisms to ensure that the magnetic filtration mechanism determines particle capture. This can be achieved by increasing particle stability. This study showed that SDS treatment stabilizes the particles. Overall, SDS treatment results in lower RE. Thus, although it provides more favorable comparisons with the trajectory model, adding SDS would not be much of an advantage to a separation process that aimed solely to remove these particles from wastewater. However, if the goal of the process is to not only remove the particles from water, but also to isolate them for the purpose of recycling and reuse, then SDS-treatment coupled with HGMS is a promising strategy. If the wastewater contained diamagnetic particles, dispersing and stabilizing these particles with SDS would decrease their removal by a ferromagnetic filter wires via non-magnetic mechanisms, while the paramagnetic particles, also stabilized, would be retained by magnetic filtration under a high applied magnetic field.

Third, optimization of a HGMS process must account for these three design factors. To achieve maximum RE the applied magnetic induction and wire thickness must be varied to achieve the strongest magnetic force, and the flow velocity must be varied to achieve the weakest drag force. However, in an industrial process, other considerations must be taken into account. A filtration process must be capable of handling sizable throughput. To achieve a high throughput, it is necessary to increase the flow rate, which also increases the fluid velocity. Operating cost is another important consideration. Generating a strong magnetic field requires electrical power, which costs money. Achieving high throughput from a magnetic filter would require a stronger magnetic field, and thus higher operating costs. Yet lowering the throughput would also raise costs, so these factors must be optimized. Thus, optimization of an HGMS process

is not a simple matter of maximizing the magnetic force while minimizing the drag force. A high throughput creates a strong drag force, which then requires a stronger magnetic force to maintain the filter performance. A higher throughput lowers operating cost while a stronger magnetic force raises operating these costs. These factors must be optimized.

Fourth, SDS-treatment could be useful for recovering particles from a magnetic filter. Often in industrial wastewater treatment operations, the contaminants are valuable materials that could be reused in the process. Therefore, it is important to be able to recover the contaminant from the filter. When filtration is due primarily to non-magnetic mechanisms, the task of recovering particles from the filter is more difficult than when filtration is due primarily to a magnetic mechanism. This is because it is more difficult to relax or reverse the attractive forces that are responsible for particle attachment. But relaxing the magnetic force is a simple matter of turning off the electromagnet. If the magnetic force is primarily responsible for particle attachment, then the particles will more readily detach when the force is removed.

CHAPTER 5

CONCLUSIONS AND RECOMMENDATIONS

A non-magnetic filtration mechanism is primarily responsible for the removal of bare Fe_2O_3 particles from water by a stainless steel filter, obscuring the effect of parameters on the RE of the filter that determine the magnitude of the forces comprising the magnetic filtration mechanism. Conversely, the magnetic filtration mechanism is primarily responsible for the removal of SDS-treated Fe_2O_3 particles. Adding SDS to the feed effectively disables the non-magnetic mechanism by increasing particle stability through a steric repulsive force. By dampening the attractive forces behind the non-magnetic mechanism, SDS-treatment accentuates the effects of these same parameters on RE, allowing for a meaningful comparison with the predictions of a trajectory model which simulates the magnetic removal mechanism.

The reliability of a trajectory model depends on including the relevant forces in the right form. This model inadequately predicts the effect of the parameters on the removal of bare Fe_2O_3 particles because it does not incorporate the appropriate non-magnetic attractive forces. However, the model predictions agree nicely with the experimental data for the removal of SDS-treated particles because the only significant attractive force is the magnetic force, which the model simulates well.

Better agreement with the predictions of a trajectory model does not justify the use of SDS in an HGMS process. If the performance of HGMS is measured by its RE, then SDS treatment is a disadvantage. However, SDS treatment can potentially improve other aspects HGMS performance. SDS treatment allows for better recovery of particles from the filter when the magnetic field is disabled, making filter regeneration much

easier. SDS treatment might also allow for selective separation of non-magnetic particles from magnetic particles. Stabilized non-magnetic particles would escape capture in a magnetic filter, while stable magnetic particles would be retained. Thus, SDS treatment has the potential to preserve two chief advantages of HGMS: the reversibility and selectivity of the magnetic force.

Future studies should focus on testing these advantages of surfactant treatment. To study how well surfactants increase the selectivity of an HGMS process, magnetic filtration experiments should be performed that measure the effect of surfactant treatment on the removal of Fe_2O_3 particles and a non-magnetic colloid, like kaolin, in the same suspension. Additional studies should examine the reversibility of the separation at higher magnetic field strengths and with different filter media. If the magnetic force is too high, the separation may not be as easily reversible. These studies could identify the optimal applied magnetic induction at which the attached particles remain in the domain of the secondary minimum potential energy, where they are easier to detach.

Also of interest would be a more thorough investigation of the effect of different types of surfactants on particle removal. Using SDS in a large scale wastewater treatment process would be infeasible economically, and undesirable environmentally. Therefore, less expensive, more environmentally friendly surfactants should be studied. Finally, in order to minimize the cost of the surfactant, the effect of surfactant concentration on reversibility and selectivity should be investigated to find an optimal concentration. This problem would also require a better understanding of the mechanism of surfactant adsorption in order to maximize adsorption. The greater the adsorption density, the less surfactant is necessary to achieve the target particle stability.

REFERENCES

Albrecht, F. (1931) *Phys. Z.*, v 32, p 48ff.

Anand, P., Etzel, J. E., Friedlaender, F. J. (1985). Heavy metals removal by high gradient magnetic separation. *IEEE Transactions on Magnetics*, v MAG-21, p 2062-2064.

Bahaj, A.S., et al. (1998) Continuous radionuclide recovery from wastewater using magnetotactic bacteria. *Journal of Magnetism and Magnetic Materials,* v 184, n 2, p 241-244.

Baker, M.N. (1949), "The Quest for Pure Water," The American Water Works Association, New York.

Barrado, E., et al. (1999) Magnetic separation of ferrite sludge from a wastewater purification process. *Water, Air and Soil Pollution*, v 115, p 385-394

Batchelor, G.K. (1970). *An Introduction to Fluid Dynamics*. Cambridge, England.

Bucak, S., et al. (2003) Protein separations using colloidal magnetic nanoparticles. *Biotechnol. Prog.,* v 19, p 477-484.

Ebner, A.D., Ritter, J.A., & Ploehn, H.J. (1997). Feasibility and limitation of nanolevel high gradient magnetic separation. *Separation and Purification Technology*, v 11, p 199-210.

Ebner, A.D., Ritter, J.A. (2001). New correlation for the capture cross section in high-gradient magnetic separation. *AIChE Journal*, v 47, p 303-313.

Gerber, R. and Birss, R. (1983). *High Gradient Magnetic Separation*. New York : Research Studies Press.

Israelachvili, Jacob (1992). *Intermolecular & Surface Forces*. 2nd edition. London: Academic Press Limited.

Kaminski, M.D. and Nunez, L. (1999). Extractant-coated magnetic particles for cobalt and nickel recovery from acidic solution." *Journal of Magnetism and Magnetic Materials,* v 194, p 31-36.

Karapinar, N. (2003) Magnetic separation of ferrihydrite from wastewater by magnetic seeding and high-gradient magnetic separation. *Int. J. Miner. Process*., v 71, p 45-54

Lawson Jr., W.F., Simons, W.H., and Treat, R.P. (1977). The dynamics of a particle attracted by a magnetized wire. *Journal of Applied Physics,* v 48, p 3213-3224.

Luborsky, F.E., and Drummond, B.J. (1976). Buildup of particle on fibers in a high field-high gradient separator. *IEEE Transactions on Magnetism, MAG-12,* 463-465.

Ma, C. and Li, C. (1989) Interaction between polyvinylpyrrolidone and sodium dodecyl sulfate at solid/liquid interface. *Journal of Colloid and Interface Science*, v131, p485-92.

Ma, C. and Li, C. (1990) Stability of dispersions of iron oxide in mixed solutions of polyvinylpyrrolidone and sodium alkyl sulfate. *Colloids and Surfaces*, v47, p117-123.

Moeser, G., et al. (2002) Water-Based Magnetic Fluids as Extractants for Synthetic Organic Compounds. *Ind. Eng. Chem. Res.*, v 414, p 739-749.

Nesset, J.E. and Finch, J.A. (1979). The static (buildup) model of particle accumulation on single wires in high gradient magnetic separation: Experimental confirmation. *IEEE Transactions on Magnetism, MAG-17*, p 1506-1509.

O'Melia, C.R. and Stumm, W. (1967) *J. Am. Water Work Assoc.* v.59, p1393ff.

Payatakes, A.C. (1973) "A New Model for Granular Porous Media: Application to Filtration for Packed Beds," Ph.D. Dissertation, Syracuse University, Syracuse, NY.

Phanapavudhikul, P., et al. (2003) Design and performance of magnetic composite particles for the separation of heavy metals from water. *Journal of Environmental Science and Health - Part A Toxic/Hazardous Substances and Environmental Engineering*, v 38, p 2277-2285.

Rajagopalan, R., and Tien, C. (1977) *Can. J. Chem. Eng.,* v 55, p 246ff.

Rosen, M. Surfactants and Interfacial Phenomena. 2nd Edition. New York: John Wiley, 1989.

Sell, W. (1931), *Ver. Deutsch. Ing. Forschungs.,* v.347, p 1ff.

Shaikh, Ahamad M.H., and Dixit, S.G. (1992) Removal of phosphate from waters by precipitation and high gradient magnetic separation. *Water Research*, v 26, n 6, p 845-852.

Somasundaran, P., et al. (1997) "Colloid Systems and Interfaces – Stability of Dispersions through Polymer and Surfactant Adsorption." Birdi, K.S., ed. *Handbook of Surface and Colloid Chemistry.* New York: CRC Press.

Svoboda, J., (1987). *Magnetic Methods for the Treatment of Minerals*. New York: Elsevier.

Tsouris, C., Yiacoumi, S., Scott, T.C. (1995). Kinetics of heterogeneous magnetic flocculation using a bivariate population-balance equation. *Chemical Engineering Communications*, 137, p 147-159.

Watson, J.H.P. (1973). Magnetic filtration. *Journal of Applied Physics,* v 44, p 4209-4213.

Yao, K.-M. (1968) "Influence of Suspended Particle Size on the Transport Aspect of Water Filtration," Ph.D. Dissertation, University of North Carolina, Chapel Hill.

Yao, K.-M., Habibian, M.T., and O'Melia, C.R. (1971). Water and Waste Water Filtration: Concepts and Applications. *Environ. Sci. Technol.*, v 5, p 1105-1112.

Ying, T.-Y., Yiacoumi, S., Tsouris, C. (2000). High-gradient magnetically seeded filtration. *Chemical Engineering Science*, v 55, p 1101-1113.